SI Appendix

The karrikin signaling regulator SMAX1 controls *Lotus japonicus* root development by suppressing ethylene biosynthesis

Samy Carbonnel, Debatosh Das, Kartikye Varshney, Markus C. Kolodziej, José A. Villaècija-Aguilar, Caroline Gutjahr*

*Correspondence to:
caroline.gutjahr@tum.de

This PDF file includes:

Supplementary Materials and Methods

Table S1 to S9

Fig. S1 to S23

www.pnas.org/cgi/doi/10.1073/pnas.2006111117

SI Materials and Methods

Plant material

Lotus japonicus wild type as well as *smax1-2, smax1-3* mutants are in the ecotype Gifu background. Mutations in SMAX1 are caused by a *LORE1* retrotransposon insertion (Table S1) and seeds, segregating for each insertion were obtained from the *Lotus* Base (https://lotus.au.dk, (1)). The *ein2a-2 ein2b-1* double mutant was kindly provided by Dugald Reid and Jens Stougaard (2). The *kai2a-1 kai2b-1* and *max2-4* mutants are described in (3).

Arabidopsis thaliana wild type as well as, *kai2-1* (4), *smax1-2 smxl2-1* (5) and *acs7-1* (NASC N16570, (6) and *ein2-1* (kindly provided by Brigitte Poppenberger) (7) are in the ecotype Columbia-0 background.

L. japonicus genotyping

Following DNA extraction, homozygous *LORE1* insertion mutants were identified by PCR by using two primer pairs: one gene-specific forward and reverse primer pair flanking the insertion site, and the second using the gene specific forward primer and the P2 primer targeting the *LORE1* sequence (Table S2).

Seed germination

L. japonicus seeds were manually scarified with sand paper, surface sterilized with 1% NaClO, washed 4 times, and incubated for 2 hours in sterile water. Imbibed seeds were germinated on half-strength Hoagland medium containing 2.5µM phosphate and 0.4% Gelrite (www.duchefa-biochemie.com), at 24°C for 3 days in the dark.

Arabidopsis thaliana seeds were surface sterilized by washing with 1 ml of 70% (v/v) ethanol and 0.05% (v/v) Triton X-100 with gentle mixing by inversion for 6 minutes at room temperature, followed by 1 wash with 96% ethanol and 5 washes with sterile distilled water. Seedlings were grown in axenic conditions on 12x12cm square plates containing 60 ml 0.5X Murashige & Skoog medium, pH5.8 (½ MS) agar-solidified medium.

Root system architecture assay

Germinated *L. japonicus* seeds were transferred onto new Petri dishes, containing half-strength Hoagland medium with 2.5µM phosphate and 0.4% Gelrite as well as

different synthetic compounds or equal amount of the solvent (Table S3) as indicated in figures, 1% sugar if indicated (Fig S6A), or two different phosphate concentrations (2.5µM and 2.5mM) (Fig S6B). Petri dishes were partially covered with black paper to keep the roots in the dark, and placed at 24°C with a 16 h light/8 h dark cycle for 2 weeks. After high-resolution scanning, post-embryonic root number was counted, and primary root length measured with Fiji (http://fiji.sc/).

For primary root length measurements of *A. thaliana* seedlings 5 and 10 days post-germination, images were obtained with a high-resolution scanner and primary root length was measured with Fiji.

Root-hair assay

To assess root hair length and distance from the root apex of *L. japonicus*, images of the primary root tips were taken of roots used for the root architecture assays. Before root-hair imaging, a Biofolie 25 film (Lumox) was placed on top of a water layer on the roots. Multiple images per root apical meristem were taken with a Leica DM6 B microscope equipped with a Leica DFC9000 GT camera. Root images were stitched using the Fiji (http://fiji.sc/) plugin MosaicJ. Fiji was used for quantification of root hair length and root hair distance from the quiescent center. Root-hair length was determined as the average of all root hairs, which were visible at their complete lengths (approximately 10-30 per plant in mock condition and 2-5 per plant with ethylene biosynthesis and perception inhibitors) in the zone of 1.5 to 2.5 mm from the root apex. For *A. thaliana* root hair length measurements, images of a minimum of 8 roots per genotype and treatment were taken with a Zeiss Discovery V8 microscope equipped with a Zeiss Axiocam 503 camera. Root hair length was measured for 10 different root hairs per root, between 2 and 3 mm from the root tip using Fiji as described (8).

Primary root thickness

Microscopy images of the primary root used to quantify root-hair phenotypes were also used to measure primary root thickness. For each plant, the width of the matured root was measured using Fiji software (http://fiji.sc/) at 3 random positions distributed across the first cm above the root tip and averaged.

Cell size determination in longitudinal root tip sections

Images of root tips were taken of the same roots used for root architecture assays. Root tips of 1 to 2 cm were fixed by vacuum infiltrating 2.5 % glutaraldehyde in 0.1M potassium phosphate buffer pH 7. After embedding in 5% low-melt agarose, sections of 45 µm were cut with a Vibratome VT1100S (Leica, Germany). Multiple images per root apical meristem samples were taken with a Leica DM6 B microscope equipped with a Leica DFC9000 GT camera. Root images were stitched using the Fiji plugin MosaicJ. Fiji was used for all quantifications, and analysis was performed in the transition zone. For cortical cell length, the cortical cell layer below the epidermis of both sides was selected as this was the most visible cell layer in the root tip. The cell lengths were measured from the first observable cell above the quiescent center and averaged with the cell at the same developmental stage on the other side of the root section. For cortical cell width, 10 random cells per root in all cortical layers were measured and averaged.

Triple response assay and hypocotyl length measurement

The triple response assay was carried out as described in Maekawa-Yoshikawa *et al.* 2009 (9) with little modifications. Seeds germinated for 2 days on 1% (v/w) Bactoagar in the dark, were rapidly transferred onto new Petri dishes, containing half-strength B5 Bactoagar medium with different concentrations of ACC and kept in dark at 24°C for additional 4 days. After high-resolution scanning, hypocotyl length (also for light grown seedlings) and thickness were measured with Fiji software (http://fiji.sc/).

SMXL degradation assay in *N. benthamiana* leaves

Nicotiana benthamiana leaves were transiently transformed by infiltration with *Agrobacterium tumefaciens* strain AGL1 as described in (10). Plasmids were constructed by Golden Gate cloning (11) as indicated in Table S5 from gene sequences amplified using Phusion PCR according to standard protocols and using primers indicated in Table S4. Fluorescent proteins were detected in *N. benthamiana* leaf epidermal cells using a confocal laser scanning microscope Leica SP5. Sequential scanning for the green (excitation: 488 nm, detection: 500-550 nm) and red fluorescence (excitation: 561 nm, detection: 570-625 nm) was carried out simultaneously with bright field image acquisition. Images were acquired using LAS AF software. Overlays were generated using Fiji (http://fiji.sc/). The number of green nuclei and red fluorescent nuclei was counted using these images or images taken on

a Leica DM6 B microscope equipped with a Leica DFC9000 GT camera using GFP and N3 filters (www.leica-microsystems.com).

Western blot

After agroinfiltration and 2 days of incubation as described for the SMXL degradation assay, three leaf discs for each plasmid were harvested for a total protein extraction. The tissue was ground into a fine powder and homogenized in 300µl lysis buffer (62.6mM Tris, 2% SDS, 10% Glycerol, 1mM DTT, 10µM Bortezomib (StressMarq Biosciences)). Samples were heated at 95°C for 5 minutes and then centrifuged at 14,000g for 30 mins at 4°C. The resulting supernatant was subjected to SDS page for Western blotting.

Proteins were separated on 10% (w/v) SDS gels and transferred to 0.45µm Immobilon®FL PVDF membranes (Millipore) using the Hoefer minigel and blotting system. Membranes were blocked in 5% skim milk powder (w/v) in PBS (pH 7.4) and probed overnight with the primary antibody rat anti-GFP to detect the SMXLs (ChromoTek, Martinsried, Germany) in 1% skim milk powder (w/v) dissolved in PBST (PBS, 0.1% Tween-20). Membranes were washed with PBST (PBS, 0.2% Tween-20) and incubated with fluorescently labelled anti-rat secondary antibody (LI-COR Biosciences, Lincoln, USA) in 1% skim milk powder (w/v) dissolved in PBST (PBS, 0.1% Tween-20) for 80 mins at 4°C. After washing, membranes were imaged by LI-COR Odyssey CLx imaging system.

Phylogenetic analysis

SMXL protein sequences were retrieved using tBLASTn with *AtSMAX1* and *OsD53* against the NCBI database and the Lotus genome V3 on *Lotus* Base (https://lotus.au.dk/). The MAFFT alignment (https://mafft.cbrc.jp) of the protein sequences was used to generate a phylogenetic tree with 1000 bootstrap replicates in IQ-TREE (12) and visualized with iTOL (https://itol.embl.de/). ACS protein sequences were retrieved using BLASTp with LjACS7 as query against Lotus genome V3 on *Lotus* Base (https://lotus.au.dk/) and TAIR (www.arabidopsis.org). The MAFFT alignment of the protein sequences was used to generate a Maximum-likelihood tree with 100 bootstrap replicates in MEGAX (13).

Seed 2D area measurement.

Seeds were randomly placed into an empty Petri dish, paying attention that the seeds did not touch each other. After a high-resolution scan, images were transformed in grey-scale 8-bit in Fiji (http://fiji.sc/). After threshold adjustment, the area was measured with the “analyze particle” tool.

Ethylene measurement

L. japonicus seedlings were grown on Petri dishes containing half-strength Hoagland medium with 2.5µM phosphate and 0.4% Gelrite, as well as 0.1µM AVG, 50µM silver nitrate, 1µM karrikin or equal amounts of solvents, and grown as described for the root architecture assay. Seven days post-germination, the seedlings were transferred into 25ml vials containing the identical medium but with only 0.2% Gelrite. Vials were sealed with rubber septa and placed into a growth chamber at 24°C with 16 h light/8 h dark cycles. After 3 days, 1ml volume of headspace was injected by syringe into a Gas Chromatograph VARIAN 3300. Ethylene peaks were recorded by an integrator Shimadzu CR6A chromatopac.

Treatment for gene expression analysis

For inducing KAR responses, seedlings grown as described for the root system architecture assay were placed for 2 hours into a half-strength Hoagland solution with 2.5µM phosphate and containing as indicated 1 or 3µM karrikin$_1$, karrikin$_2$, *rac*-GR24, or equal amounts of the corresponding solvents (Table S3). For ethylene signaling inhibition, seedlings were grown for 10 days on half-strength Hoagland solution with 2.5µM phosphate and 0.4 % Gelrite containing 0.1µM AVG or 50µM silver nitrate.

Transcript accumulation analysis by RT-qPCR

Transcript accumulation analysis in *Lotus japonicus* roots by quantitative RT-PCR was performed as described (3). For Arabidopsis RT-qPCR analysis, a minimum of 100 roots per sample was rapidly shock frozen in liquid nitrogen. RNA was extracted using NucleoSpin RNA plant and fungi kit (Macherey-Nagel). The concentration and purity of RNA was evaluated with DS-11 FX+ spectrophotometer/fluorometer (DeNovix). First-strand cDNA was produced in a 20 µL reaction volume using the Superscript IV kit (Invitrogen). The cDNA was diluted with water in a 1:20 ratio and 1 µL of this solution was used for RT-qPCR in a 20 µL reaction volume using a Green MasterMix (Jena Bioscience, highROX, 2x conc.). To quantify the expression of the different

genes, the qPCR reaction was carried out using a LightCycler 480 RT-PCR detection system (Roche). Thermal cycler conditions were: 95°C 2 min, 40 cycles of 95°C 30s, 55°C 30s and 72°C 20 s, followed by dissociation curve analysis. For the calculation of the expression levels, we followed the ΔΔCt method (14). Each sample of three biological replicates per genotype was represented by 3 technical replicates. Primers are indicated in Table S6.

Transcript accumulation analysis by RNAseq

Root tissue was harvested and rapidly shock-frozen in liquid nitrogen. RNA was extracted using the Spectrum Plant Total RNA Kit (Sigma). DNA was removed by DNAse I treatment on column (Sigma). Residual DNA was removed by LiCl precipitation. The RNA purity was tested by PCR. The RNA quality was tested on an Agilent Bioanalyzer, and samples with RIN>6.7 were processed further. Libraries were created with TruSeq® Stranded mRNA LT (RS-122-2101, Illumina) after selection with AMPure XP beads (NEB). Sequencing was performed on a HISeq 2500 with 2x100bp paired-end (Illumina). Raw fastq files obtained from the sequencing facility were tested for quality with FastQC (Babraham Institute). Data were processed with quasi-transcript mapping approach in Salmon (15). Salmon was operated in Conda environment inside the Linux terminal (https://anaconda.org/bioconda/salmon). One replicate of *smax1-2* RNA was found to have strongly reduced number of reads and was removed from further analysis (Fig. S9, S10). Reads were mapped onto the *L. japonicus* MG20 mRNA version 3.0 reference (Lotusjaponicus_MG20_v3.0_cdna.fa) downloaded from *Lotus* Base (16). Read counts were obtained for *L. japonicus* transcripts at the gene level. Read counts were further processed through tximport in R/Bioconductor (17) for input into DESeq2 for data exploratory analysis and differential expression analysis (wild-type versus mutants), with adjusted p-value ≤ 0.01 and LogFC $\geq |0.5|$ thresholds. Heatmaps were prepared using the pheatmap package in R/Bioconductor (17). AgriGO was utilized to find enriched GO terms for the differentially expressed genes (18). The RNAseq analysis workflow is shown in Fig. S8.

Statistical analysis

Statistical analyses were performed using R statistical environment (https://www.r-project.org/). For equal variance, gene expression and ethylene measurement data

were log transformed prior to analysis. Statistical results of the ANOVAs are indicated in Table S7.

Supplementary Tables

Table S1. *L. japonicus* and *Arabidopsis thaliana* mutants used in this study.

allele	type	Line	position from ATG	comments
kai2a-1	*LORE1* insertion	30008990	387	Described in (3)
kai2b-1	EMS	SL1281	C640T (Q > stop)	
max2-4	*LORE1* insertion	30049531	1230	
smax1-1	*LORE1* insertion	30056261	498	No germination
smax1-2	*LORE1* insertion	30039146	601	
smax1-3	*LORE1* insertion	30015424	917	
ein2a-2 ein2b-1	*LORE1* insertions	Described in (2)		
Atkai2-1	EMS	Described in (4)		
Atacs7-1	T-DNA insertion	Described in (6)		
Atein2-1	EMS	Described in (7)		
Atsmax1-2 smxl2-1	T-DNA insertion	Described in (19)		

Table S2. Primers used for *LORE1* insertion mutant genotyping. Presence of the *LORE1* insertion was detected using the forward primer and the *LORE1* specific primer CCATGGCGGTTCCGTGAATCTTAGG.

allele	Forward		Reverse	
smax1-1	Sc189	CGACGCTTCTAGCTTCGC CGTCTG	Sc190	CACATGGCCATTGCTGA AAACCCC
smax1-2	Sc191	CACATGGCCATTGCTGAAA ACCCC	Sc192	CGACGCTTCTAGCTTCGCC GTCTG
smax1-3	Sc193	GGCACTGCCTGAAGATCCC AATCA	Sc194	TACCGCGCCGAGCAGGAA TTTGTA

Table S3. Signaling compounds and inhibitors.

compound	Supplier	Solvent	Stock Concentration
$Karrikin_1$	Olchemim	75% Methanol	10 mM
$Karrikin_2$	Olchemim	75% Methanol	10 mM

rac-GR24	Chiralix	100% Acetone	10 mM
ACC	Sigma	water	10 mM
Ethephon	Sigma	water	10 mM
AVG	Sigma	water	10 mM
Silver nitrate	Sigma	water	50 mM

Table S4. Cloning primers.

Plasmid	**Primers**	
LI *gLjD14* wo ATG	MK1	AAGGTCTCACACCGCCACTTCAATCCTCGAC
	Sc12	TTGAAGACTACAGAGGTCTCTCCTTTCAGTGTGCCCCCGCCAGTG
LI *gLjKAI2a* wo ATG	MK2	AAGGTCTCACACCGGGATAGTGGAGGAAGCTCA
	Sc14	TTTGGTCTCTCCTTTTACACCCCACTAAATTTTACATCAC
LI *gLjKAI2b* wo ATG	MK3	AAGGTCTCACACCGGGATAGTGGAAGAAGCTCAC
	Sc18	TTGAAGACTACAGAGGTCTCTCCTTTCAAGCTGCAATATCATGGCAAATG
LI *gLjMAX2* wo ATG	MK4	AAGGTCTCACACCAGTAACGCTGCTGAAACCAC
	Sc137	ATGAAGACTTCAGAGGTCTCACCTTTCAATCACAGATATGACGC
LI Esp3i *LjSMAX1* A	Sc249	TTTCGTCTCACACCATGAGAGCGGGTCTCAGCACCATCC
	Sc274	TTTCGTCTCATAGTTCCGCATACACTGGGGA
LI Esp3i *LjSMAX1* B	Sc275	TTTCGTCTCAACTACGAGCAAGAAGTAGCAGAAATG
	Sc250	TTTCGTCTCACCTTACACTGTTCCGCCACCAGTCTC
LI Esp3i *gLjSMXL3* A	MK5	TATCGTCTCACACCATGAGAACTGGAAACTGTGCTG
	MK6	TATCGTCTCAGTAGTTGCTTTATTCTCATTCTTATACTG
LI Esp3i *gLjSMXL3* B	MK7	TATCGTCTCACTACCTACAATCATCAGGTCTTGA
	MK8	TATCGTCTCACCTTTAAGTTCTGAAATTTGAAGATAAACATT
LI Esp3i *gLjSMXL4* A	MK13	TATCGTCTCACACCATGCGCTCAGGAGCTTG
	MK14	TATCGTCTCAGTGCTTCTTTTTCATAATTTGAGG
LI Esp3i *gLjSMXL4* B	MK15	TATCGTCTCAGCACAGTTGTTCAAACCAGG
	MK16	TATCGTCTCACCTTATCCATGAAGTAGTTAACTTGGATG
LI Esp3i *gLjSMXL9* A	MK9	TATCGTCTCACACCATGAGGGGAGGAATTTGC
	MK10	TATCGTCTCACTCCTACTCTATCTTCAAAAGGCA
LI Esp3i *gLjSMXL9* B	MK11	TATCGTCTCAGGAGCAAGGAAGAATCTAACTTG
	MK12	TATCGTCTCACCTTAAAGTTAAAACTAATTTGCTTATCAACTAAC
LI Esp3i *gLjSMXL8* A	Sc253	TTTCGTCTCACACCATGCCAACGCCGGTAGGAGTAG
	Sc254	TTTCGTCTCATCTCCACTCTCCACCTCCTTCC
LI Esp3i *gLjSMXL8* B	Sc255	TTTCGTCTCAGAGATGGCGAGGCCGTCGGTGC
	Sc276	TTTCGTCTCACCACGGAAGCAGAAAAGA
	Sc277	TTTCGTCTCAGTGGCTGATCCCTACCAATCT

LI Esp3i *gLjSMXL8* C	Sc256	TTTCGTCTCATCTGGATCGCAAAATTCATTGTC
LI Esp3i *gLjSMXL8* D	Sc257	TTTCGTCTCACAGAAACGCCTAAAAGGGCACATACA
	Sc258	TTTCGTCTCACCTTTTCTACAATTATCCTTGGAGGAAGG
LI Esp3i *LjSMAX1^{d53}* A	Sc249	TTTCGTCTCACACCATGAGAGCGGGTCTCAGCACCATCC
	Sc251	TTTCGTCTCAGTGAGATGGTTAACTTCAGAG
LI Esp3i *LjSMAX1^{d53}* B	Sc252	TTTCGTCTCATCACTGATCGGATTGCTGAGGCCATC
	Sc250	TTTCGTCTCACCTTACACTGTTCCGCCACCAGTCTC
LI Esp3i *gLjSMXL8^{d53}* C'	Sc277	TTTCGTCTCAGTGGCTGATCCCTACCAATCT
	Sc259	TTTCGTCTCATGAATTTGACATTGCATCCTTTC
LI Esp3i *gLjSMXL8^{d53}* C''	Sc260	TTTCGTCTCATTCACTGATTTTATTGTGAGGGAGTATTGC
	Sc256	TTTCGTCTCATCTGGATCGCAAAATTCATTGTC

Table S5. Plasmids.

Name	**Description**	**Cut ligation**
Golden Gate Level I		
LI *gLjD14* wo ATG	PCR amplification of LI gLjD14 (Carbonnel et al., 2019) with primers MK1 and Sc12. Assembly into LI-pUC57 (BB02)	StuI
LI *gLjKAI2a* wo ATG	PCR amplification of LI gLjKAI2a (Carbonnel et al., 2019) with primers MK2 and Sc14. Assembly into LI-pUC57 (BB02)	StuI
LI *gLjKAI2b* wo ATG	PCR amplification of LI gLjKAI2b (Carbonnel et al., 2019) with primers MK3 and Sc18. Assembly into LI-pUC57 (BB02)	StuI
LI *gLjMAX2* wo ATG	PCR amplification of LI gLjMAX2 (Carbonnel et al., 2019) with primers MK4 and Sc137. Assembly into LI-pUC57 (BB02)	StuI
LI Esp3i *LjSMAX1* A	PCR amplification of *L. japonicus* Gifu genomic DNA with primers Sc249 and Sc274. Assembly into LI-pUC57 (BB02)	StuI
LI Esp3i *LjSMAX1* B	PCR amplification of *L. japonicus* Gifu genomic DNA with primers Sc275 and Sc250. Assembly into LI-pUC57 (BB02)	StuI
LI Esp3i *gLjSMXL3* A	PCR amplification of *L. japonicus* Gifu genomic DNA with primers MK5 and MK6. Assembly into LI-pUC57 (BB02)	SmaI
LI Esp3i *gLjSMXL3* B	PCR amplification of *L. japonicus* Gifu genomic DNA with primers MK7 and MK8. Assembly into LI-pUC57 (BB02)	SmaI
LI Esp3i *gLjSMXL4* A	PCR amplification of *L. japonicus* Gifu genomic DNA with primers MK13 and MK14. Assembly into LI-pUC57 (BB02)	SmaI
LI Esp3i *gLjSMXL4* B	PCR amplification of *L. japonicus* Gifu genomic DNA with primers MK15 and MK16. Assembly into LI-pUC57 (BB02)	SmaI
LI Esp3i *gLjSMXL9* A	PCR amplification of *L. japonicus* Gifu genomic DNA with primers MK9 and MK10. Assembly into LI-pUC57 (BB02)	SmaI
LI Esp3i *gLjSMXL9* B	PCR amplification of *L. japonicus* Gifu genomic DNA with primers MK11 and MK12. Assembly into LI-pUC57 (BB02)	SmaI
LI Esp3i *gLjSMXL8* A	PCR amplification of *L. japonicus* Gifu genomic DNA with primers Sc253 and Sc254. Assembly into LI-pUC57 (BB02)	StuI
LI Esp3i *gLjSMXL8* B	PCR amplification of *L. japonicus* Gifu genomic DNA with primers Sc255 and Sc276. Assembly into LI-pUC57 (BB02)	StuI

LI Esp3i *gLjSMXL8* C	PCR amplification of *L. japonicus* Gifu genomic DNA with primers Sc277 and Sc256. Assembly into LI-pUC57 (BB02)	StuI
LI Esp3i *gLjSMXL8* D	PCR amplification of *L. japonicus* Gifu genomic DNA with primers Sc257 and Sc258. Assembly into LI-pUC57 (BB02)	StuI
LI Esp3i *LjSMAX1^{d53}* A	PCR amplification of *L. japonicus* Gifu genomic DNA with primers Sc249 and Sc251. Assembly into LI-pUC57 (BB02)	StuI
LI Esp3i *LjSMAX1^{d53}* B	PCR amplification of *L. japonicus* Gifu genomic DNA with primers Sc252 and Sc250. Assembly into LI-pUC57 (BB02)	StuI
LI Esp3i *gLjSMXL8^{d53}* C'	PCR amplification of *L. japonicus* Gifu genomic DNA with primers Sc277 and Sc259. Assembly into LI-pUC57 (BB02)	StuI
LI Esp3i *gLjSMXL8^{d53}* C''	PCR amplification of *L. japonicus* Gifu genomic DNA with primers Sc260 and Sc256. Assembly into LI-pUC57 (BB02)	StuI
Golden Gate Level II		
LIIc F1-2 *pUbi:*GOI*_GFP*	Assembled from: LI *pUbi* (G7) + LI B-C dy (BB06) + LI dy POI (G83) + LI D-E *GFP* (G11) + LI E-F nos-T (G6) + LI F-G dy (BB09) + LIIc F 1-2 (BB30)	BsaI
LIIc R3-4 p*35S:mCherry*	Assembled from: LI A-B p*35S* (G005) + LI B-C dy (BB06) + LI C-D *mCherry* (G023) + LI D-E dy (BB08) + LI E-F 35S-T (G059) + LI F-G dy (BB09) + LIIc R 3-4 (BB34)	BsaI
LIIc F4-5 *pUbi:HA_gLjD14*	Assembled from: LI A-B *pUbi* (G7) + LI B-C *HA* (G67) + LI C-D *gLjD14* wo ATG+ LI D-E dy (BB8) + LI E-F HSP-T (G45) + LI F-G dy (BB09) + LIIc F4-5 (BB35)	BsaI
LIIc F4-5 *pUbi:HA_gLjKAI2a*	Assembled from: LI A-B *pUbi* (G7) + LI B-C *HA* (G67) + LI C-D *gLjKAI2a* wo ATG + LI D-E dy (BB8) + LI E-F HSP-T (G45) + LI F-G dy (BB09) + LIIc F4-5 (BB35)	BsaI
LIIc F4-5 *pUbi:HA_gLjKAI2b*	Assembled from: LI A-B *pUbi* (G7) + LI B-C *HA* (G67) + LI C-D *gLjKAI2b* wo ATG + LI D-E dy (BB8) + LI E-F HSP-T (G45) + LI F-G dy (BB09) + LIIc F4-5 (BB35)	BsaI
LIIc F5-6 p*35S:MYC_MAX2*	Assembled from: LI A-B p*35S* (G005) + LI B-C *MYC* (G069) + LI C-D *gLjMAX2* wo ATG + LI D-E dy (BB08) + LI E-F 35S-T (G059) + LI F-G dy (BB09) + LIIc F5-6 (BB37)	BsaI
Golden Gate Level III		
LIIIβ *pUbi:*GOI*_GFP* p*35S:mCherry* *pUbi:HA_gLjD14* p*35S:MYC_MAX2*	Assembled from: LIIc F 1-2 *pUbi:*GOI*_GFP* + LII 2-3 ins (BB43) + LIIc R 3-4 p35S:*mCherry* + LII 4-5 *pUbi:HA_gLjD14* + LII 5-6 p*35S:MYC_MAX2* + LIIIβ F A-B (BB53)	BpiI
LIIIβ *pUbi:*GOI*_GFP* p*35S:mCherry* *pUbi:HA_gLjKAI2a* p*35S:MYC_MAX2*	Assembled from: LIIc F 1-2 *pUbi:*GOI*_GFP* + LII 2-3 ins (BB43) + LIIc R 3-4 p35S:*mCherry* + LII 4-5 *pUbi:HA_gLjKAI2a* + LII 5-6 p*35S:MYC_MAX2* + LIIIβ F A-B (BB53)	BpiI
LIIIβ *pUbi:*GOI*_GFP* p*35S:mCherry* *pUbi:HA_gLjKAI2b* p*35S:MYC_MAX2*	Assembled from: LIIc F 1-2 *pUbi:*GOI*_GFP* + LII 2-3 ins (BB43) + LIIc R 3-4 p35S:*mCherry* + LII 4-5 *pUbi:HA_gLjKAI2b* + LII 5-6 p*35S:MYC_MAX2* + LIIIβ F A-B (BB53)	BpiI
LIIIβ *pUbi:gLjSMAX1_GFP* p*35S:mCherry* *pUbi:HA_gLjD14* p*35S:MYC_MAX2*	Assembled from: LIIIβ *pUbi:*GOI*_GFP* p*35S:mCherry* *pUbi:HA_gLjD14* p*35S:MYC_MAX2* + LI Esp3I *gLjSMAX1* A + LI Esp3I *gLjSMAX1* B	Esp3I
LIIIβ *pUbi:gLjSMAX1_GFP* p*35S:mCherry* *pUbi:HA_gLjKAI2a* p*35S:MYC_MAX2*	Assembled from: LIIIβ *pUbi:*GOI*_GFP* p*35S:mCherry* *pUbi:HA_gLjKAI2a* p*35S:MYC_MAX2* + LI Esp3I *gLjSMAX1* A + LI Esp3I *gLjSMAX1* B	Esp3I

LIIIβ *pUbi:gLjSMAX1_GFP* p*35S:mCherry* *pUbi:HA_gLjKAI2b* p*35S:MYC_MAX2*	Assembled from: LIIIβ *pUbi:*GOI*_GFP* p*35S:mCherry* *pUbi:HA_gLjKAI2b* p*35S:MYC_MAX2* + LI Esp3I *gLjSMAX1* A + LI Esp3I *gLjSMAX1* B	Esp3I
LIIIβ *pUbi:gLjSMXL3_GFP* p*35S:mCherry* *pUbi:HA_gLjD14* p*35S:MYC_MAX2*	Assembled from: LIIIβ *pUbi:*GOI*_GFP* p*35S:mCherry* *pUbi:HA_gLjD14* p*35S:MYC_MAX2* + LI Esp3I *gLjSMXL3* A + LI Esp3I *gLjSMXL3* B	Esp3I
LIIIβ *pUbi:gLjSMXL3_GFP* p*35S:mCherry* *pUbi:HA_gLjKAI2a* p*35S:MYC_MAX2*	Assembled from: LIIIβ *pUbi:*GOI*_GFP* p*35S:mCherry* *pUbi:HA_gLjKAI2a* p*35S:MYC_MAX2* + LI Esp3I *gLjSMXL3* A + LI Esp3I *gLjSMXL3* B	Esp3I
LIIIβ *pUbi:gLjSMXL3_GFP* p*35S:mCherry* *pUbi:HA_gLjKAI2b* p*35S:MYC_MAX2*	Assembled from: LIIIβ *pUbi:*GOI*_GFP* p*35S:mCherry* *pUbi:HA_gLjKAI2b* p*35S:MYC_MAX2* + LI Esp3I *gLjSMXL3* A + LI Esp3I *gLjSMXL3* B	Esp3I
LIIIβ *pUbi:gLjSMXL9_GFP* p*35S:mCherry* *pUbi:HA_gLjD14* p*35S:MYC_MAX2*	Assembled from: LIIIβ *pUbi:*GOI*_GFP* p*35S:mCherry* *pUbi:HA_gLjD14* p*35S:MYC_MAX2* + LI Esp3I *gLjSMXL9* A + LI Esp3I *gLjSMXL9* B	Esp3I
LIIIβ *pUbi:gLjSMXL9_GFP* p*35S:mCherry* *pUbi:HA_gLjKAI2a* p*35S:MYC_MAX2*	Assembled from: LIIIβ *pUbi:*GOI*_GFP* p*35S:mCherry* *pUbi:HA_gLjKAI2a* p*35S:MYC_MAX2* + LI Esp3I *gLjSMXL9* A + LI Esp3I *gLjSMXL9* B	Esp3I
LIIIβ *pUbi:gLjSMXL9_GFP* p*35S:mCherry* *pUbi:HA_gLjKAI2b* p*35S:MYC_MAX2*	Assembled from: LIIIβ *pUbi:*GOI*_GFP* p*35S:mCherry* *pUbi:HA_gLjKAI2b* p*35S:MYC_MAX2* + LI Esp3I *gLjSMXL9* A + LI Esp3I *gLjSMXL9* B	Esp3I
LIIIβ *pUbi:gLjSMXL4_GFP* p*35S:mCherry* *pUbi:HA_gLjD14* p*35S:MYC_MAX2*	Assembled from: LIIIβ *pUbi:*GOI*_GFP* p*35S:mCherry* *pUbi:HA_gLjD14* p*35S:MYC_MAX2* + LI Esp3I *gLjSMXL4* A + LI Esp3I *gLjSMXL4* B	Esp3I
LIIIβ *pUbi:gLjSMXL4_GFP* p*35S:mCherry* *pUbi:HA_gLjKAI2a* p*35S:MYC_MAX2*	Assembled from: LIIIβ *pUbi:*GOI*_GFP* p*35S:mCherry* *pUbi:HA_gLjKAI2a* p*35S:MYC_MAX2* + LI Esp3I *gLjSMXL4* A + LI Esp3I *gLjSMXL4* B	Esp3I
LIIIβ *pUbi:gLjSMXL4_GFP* p*35S:mCherry* *pUbi:HA_gLjKAI2b* p*35S:MYC_MAX2*	Assembled from: LIIIβ *pUbi:*GOI*_GFP* p*35S:mCherry* *pUbi:HA_gLjKAI2b* p*35S:MYC_MAX2* + LI Esp3I *gLjSMXL4* A + LI Esp3I *gLjSMXL4* B	Esp3I
LIIIβ *pUbi:gLjSMXL8_GFP* p*35S:mCherry* *pUbi:HA_gLjD14* p*35S:MYC_MAX2*	Assembled from: LIIIβ *pUbi:*GOI*_GFP* p*35S:mCherry* *pUbi:HA_gLjD14* p*35S:MYC_MAX2* + LI Esp3I *gLjSMXL8* A + LI Esp3I *gLjSMXL8* B + LI Esp3I *gLjSMXL8* C + LI Esp3I *gLjSMXL8* D	Esp3I
LIIIβ *pUbi:gLjSMXL8_GFP* p*35S:mCherry* *pUbi:HA_gLjKAI2a* p*35S:MYC_MAX2*	Assembled from: LIIIβ *pUbi:*GOI*_GFP* p*35S:mCherry* *pUbi:HA_gLjD14* p*35S:MYC_MAX2* + LI Esp3I *gLjSMXL8* A + LI Esp3I *gLjSMXL8* B + LI Esp3I *gLjSMXL8* C + LI Esp3I *gLjSMXL8* D	Esp3I
LIIIβ *pUbi:gLjSMXL8_GFP* p*35S:mCherry* *pUbi:HA_gLjKAI2b*	Assembled from: LIIIβ *pUbi:*GOI*_GFP* p*35S:mCherry* *pUbi:HA_gLjD14* p*35S:MYC_MAX2* + LI Esp3I *gLjSMXL8* A + LI Esp3I *gLjSMXL8* B + LI Esp3I *gLjSMXL8* C + LI Esp3I *gLjSMXL8* D	Esp3I

p*35S:MYC_MAX2*		
LIIIβ *pUbi:*GOI*_GFP* p*35S:mCherry pUbi:HA_gLjD14*	Assembled from: LIIc F 1-2 *pUbi:*GOI*_GFP* + LII 2-3 ins (BB43) + LIIc R 3-4 p35S:*mCherry* + LII 4-5 *pUbi:HA_gLjD14* + LII 5-6 *dy* (BB65) + LIIIβ F A-B (BB53)	BpiI
LIIIβ *pUbi:*GOI*_GFP* p*35S:mCherry pUbi:HA_gLjKAI2a*	Assembled from: LIIc F 1-2 *pUbi:*GOI*_GFP* + LII 2-3 ins (BB43) + LIIc R 3-4 p35S:*mCherry* + LII 4-5 *pUbi:HA_gLjKAI2a* + LII 5-6 *dy* (BB65)+ LIIIβ F A-B (BB53)	BpiI
LIIIβ *pUbi:*GOI*_GFP* p*35S:mCherry pUbi:HA_gLjKAI2b*	Assembled from: LIIc F 1-2 *pUbi:*GOI*_GFP* + LII 2-3 ins (BB43) + LIIc R 3-4 p35S:*mCherry* + LII 4-5 *pUbi:HA_gLjKAI2b* + LII 5-6 *dy* (BB65)+ LIIIβ F A-B (BB53)	BpiI
LIIIβ *pUbi:SMXL8_GFP* p*35S:mCherry pUbi:HA_gLjD14*	Assembled from: LIIIβ *pUbi:*GOI*_GFP* p*35S:mCherry pUbi:HA_gLjD14* + LI Esp3I *gLjSMXL8* A + LI Esp3I *gLjSMXL8* B + LI Esp3I *gLjSMXL8* C + LI Esp3I *gLjSMXL8* D	Esp3I
LIIIβ *pUbi:SMAX1_GFP* p*35S:mCherry pUbi:HA_gLjKAI2a*	Assembled from: LIIIβ *pUbi:*GOI*_GFP* p*35S:mCherry pUbi:HA_gLjKAI2a* + LI Esp3I *gLjSMAX1* A + LI Esp3I *gLjSMAX1* B	Esp3I
LIIIβ *pUbi:SMAX1_GFP* p*35S:mCherry pUbi:HA_gLjKAI2b*	Assembled from: LIIIβ *pUbi:*GOI*_GFP* p*35S:mCherry pUbi:HA_gLjKAI2b* + LI Esp3I *gLjSMAX1* A + LI Esp3I *gLjSMAX1* B	Esp3I
LIIIβ *pUbi:gLjSMAX1^{d53}_GFP* p*35S:mCherry pUbi:HA_gLjKAI2a* p*35S:MYC_MAX2*	Assembled from: LIIIβ *pUbi:*GOI*_GFP* p*35S:mCherry pUbi:HA_gLjKAI2a* p*35S:MYC_MAX2* + LI Esp3I *gLjSMAX1d53* A + LI Esp3I *gLjSMAX1d53* B	Esp3I
LIIIβ *pUbi:gLjSMAX1^{d53}_GFP* p*35S:mCherry pUbi:HA_gLjKAI2b* p*35S:MYC_MAX2*	Assembled from: LIIIβ *pUbi:*GOI*_GFP* p*35S:mCherry pUbi:HA_gLjKAI2b* p*35S:MYC_MAX2* + LI Esp3I *gLjSMAX1d53* A + LI Esp3I *gLjSMAX1d53* B	Esp3I
LIIIβ *pUbi:gLjSMXL8^{d53}_GFP* p*35S:mCherry pUbi:HA_gLjD14* p*35S:MYC_MAX2*	Assembled from: LIIIβ *pUbi:*GOI*_GFP* p*35S:mCherry pUbi:HA_gLjD14* p*35S:MYC_MAX2* + LI Esp3I *gLjSMXL8* A + LI Esp3I *gLjSMXL8* B + LI Esp3I *gLjSMXL8^{d53}* C' + LI Esp3I *gLjSMXL8^{d53}* C'' + LI Esp3I *gLjSMXL8* D	Esp3I

Table S6. qPCR primers and RT PCR primers.

Use	**Primers**	
RT-PCR 5' *SMAX1*	KV87	TCTCATCCCAATTCCTCTCATC
	KV88	TTCAAGGCCGCCATCAAAG
RT-PCR flanking *smax1-2*	KV95	TTCCTTCCGCCGTGAATTCC
	KV96	TATCCACCACCCGTTTCACC
RT-PCR flanking *smax1-3*	KV97	TGATTCATTTGGAGAAGGAGC
	KV98	CAAACCACCAACCCCAAAC
RT-PCR 3' *SMAX1* and qPCR *SMAX1*	Sc114	TGACAAGATTGCCAGTGGAG
	Sc115	CTAACCAGCAGCGAACAAGAC
	Ubi F	ATGCAGATCTTCGTCAAGACCTTG

RT-PCR and qPCR *Ubiquitin*	Ubi R	ACCTCCCCTCAGACGAAG
qPCR *DLK2*	MG027	CTCCTTGGTGCTTCTCCCAG
	MG028	AAAGCCGAAGCCAGTTTTCA
qPCR *SMXL3*	Sc138	GAAATTGCAAGCACCGTTTT
	Sc139	TCTGCGAAACTGCTCAGAGA
qPCR *SMXL9*	Sc140	TCTCTGTGATGCCTTGGAGA
	Sc141	TCTTTGGCCTGAGAATCCAC
qPCR *SMXL4*	Sc142	CAAGAGAAGGGCTGAACTGG
	Sc143	AGGGATCGGCTATGGTTTCT
qPCR *SMXL7a*	Sc112	GAGGTAATGGCACAGATACTCG
	Sc113	AGGGTGGGTTTTCTGCTTAG
qPCR *SMXL7b*	Sc144	TGCATGGTTATCGGACAAGA
	Sc145	AGCTGGAAGGCACACTCCTA
qPCR *SMXL8*	Sc146	CCAAAGCATCAGTGCAGCTA
	Sc147	ACAAACCTTGCAACCAAAGG
qPCR *ERF* (*Lj2g3v1068730*)	Sc507	ACCTGAGTGCTTGAAGTTCAC
	Sc508	CCCTTGCTGCCATCATGTAC
qPCR *Germin-like* (*Lj3g3v2601420*)	Sc509	CCCTGGCCTTCAAATCCTTG
	Sc510	TGCCACCAAGAACACCCTTA
qPCR *Serotonin receptor-like* (*Lj4g3v0496580*)	Sc523	AGCACTGTCAAGCACTACCT
	Sc524	TCCACTACCCGTTGTTTCGA
qPCR *IAMT1-like* (*Lj2g3v3222870*)	Sc527	AACATTCCGGTTTATGCGCC
	Sc528	GCCCTGCCTACTTCACTAGC
qPCR *auxin-induced 5NG4-like* (*Lj6g3v2244450*)	Sc533	TGCGTCTGTTTTCAACCCTC
	Sc534	CCATGTACAAGCCACACACA
qPCR *coatomer subunit Beta-2-like (Lj3g3v0139630)*	Sc577	GGTCTGGAGAGAGTGTGGAG
	Sc578	TGGCAGCTTCCAGATTCAGT
qPCR *Lj0g3v0127589*	Sc575	CCAAACATGCTAACCGGTGT
	Sc576	CTTGCTTCTTGTGCTGTCCA
qPCR *CLAVATA3-like (Lj3g3v0428680)*	Sc581	AGTTCTGGCATTGCTTGTGG
	Sc582	GGTGACACTCTCTCAAGCCT
qPCR *P450 N-monooxoagenase2 (Lj3g3v0744710)*	Sc525	TGATGGCTTGAAGACCGTTG
	Sc526	TTGCGCCTTGATTTCCTTCA
qPCR *Salt-tolerance-like (Lj1g3v3370960)*	Sc519	TCCCTGGTTACTGCTTCGAA
	Sc520	CGAATGGCTAAGTTGAGGGG
qPCR *ACC Synthase (Lj2g3v0909590)*	Sc595	CGCTCGGAGGATGTCAAGTT
	Sc596	CCCTGCATTCCCTTCCAAGT
qPCR *ACC Oxidase (Lj3g3v0652730)*	Sc593	TGGTCCATTGCCTCAAGTCC
	Sc594	AGCATGTTCAATGGTCGCCT

qPCR *Expansin (Lj0g3v0287409)*	Sc601	CGGGGATGTGAAGGCTGTAT
	Sc602	CTGGTTTCTGAGGTCTGCGT
qPCR *Acid Phosphatase (Lj3g3v3640290)*	Sc591	GCTGTTATTGGCATGGCTGG
	Sc592	AACTGTCCTTAACTTCCCTGGT
qPCR *NBS-LRR (Lj4g3v3113360)*	Sc563	AGCCAGCTTTCACGGTAAAA
	Sc564	TAGTCACCAGCAACGCCATA
qPCR *Basic-leucine-zipper TF (Lj0g3v0268559)*	Sc561	TGATGCCATGGGAAGGAAAC
	Sc562	TCCAAACATGCATGCAGTGT
qPCR *somatic embryogenesis RLK1 (Lj0g3v0241899)*	Sc569	TGGATCTGTGTGGACCAGTC
	Sc570	GACACATGGAGGAGGAGGAG
qPCR *RLK (Lj6g3v1370760)*	Sc571	CTGGACAACTTGGGGAGCTA
	Sc572	GGCTTGGGAATTTCATCGGA
qPCR *Trichome birefringence-like 27 (Lj0g3v0194729)*	Sc535	AGAGGAAAGCAGCTCAAGGA
	Sc536	CACCCTTATCCCACGAACCT
qPCR *AtDLK2* (AT3G24420) (4)	DLK2-F	GAAATCAACCGCCCAAGCT
	DLK2-R	GAAATCAACCGCCCAAGCT
qPCR *AtACS7* (AT4G26200)	ACS7-F	CCGTATTATCCAGGATTCGAT
	ACS7-R	CTTTTGGACCGTCGCCCCTA

Table S7: Statistical results of ANOVA.

Figure	condition	P value	F value
Fig 2B	PR length	≤ 0.001	$F_{2/106} = 39.3$
	PER number	= 0.26	$F_{2/106} = 1.37$
	PER density	≤ 0.001	$F_{2/106} = 20.3$
Fig 2C	PRL	≤ 0.001	$F_{2/69} = 10.4$
	PER	≤ 0.001	$F_{2/69} = 8.1$
	PER density	≤ 0.001	$F_{2/69} = 23.8$
Fig 2E	-	≤ 0.01	$F_{2/19} = 8.47$
Fig 2F	-	≤ 0.001	$F_{2/19} = 12.5$
Fig 3B	-	≤ 0.001	$F_{4/14} = 230.7$
Fig 3C	-	≤ 0.001	$F_{4/14} = 39.7$
Fig 4A	-	≤ 0.001	$F_{8/36} = 174.9$
Fig 4C	PR length	≤ 0.001	$F_{5/169} = 73.3$
	PER number	≤ 0.001	$F_{5/169} = 26.2$
	PER density	≤ 0.001	$F_{5/169} = 30.7$
Fig 4E	-	≤ 0.001	$F_{5/43} = 19.1$
Fig 4F	-	≤ 0.001	$F_{5/42} = 122.6$
Fig S5B	-	≤ 0.001	$F_{2/225} = 315.3$
Fig S5C	-	= 0.054	$F_{2/9} = 4.12$
Fig S5D	-	≤ 0.01	$F_{2/9} = 8.4$

Fig S6A	PR length	≤ 0.001	$F_{3/182} = 96.2$
	PER number	≤ 0.05	$F_{3/182} = 3.83$
	PER density	≤ 0.001	$F_{3/182} = 45.8$
Fig S7B	-	≤ 0.001	$F_{3/32} = 45.6$
Fig S7C	-	≤ 0.001	$F_{3/32} = 33.5$
Fig S7A	-	≤ 0.001	$F_{4/28} = 21.3$
Fig S7B	-	≤ 0.001	$F_{4/28} = 36.1$
Fig S8A	PR length	≤ 0.001	$F_{5/319} = 272.3$
	PER number	≤ 0.001	$F_{5/319} = 66.3$
	PER density	≤ 0.001	$F_{5/319} = 28.8$
Fig S8B	PR length	≤ 0.001	$F_{3/136} = 87.4$
	PER number	≤ 0.001	$F_{3/136} = 17.5$
	PER density	≤ 0.001	$F_{3/136} = 22$
Fig S13	*Germin-like*	≤ 0.001	$F_{4/14} = 36.9$
	Coatomer-subunit-beta-2-like	≤ 0.001	$F_{4/14} = 21.3$
	Unknown	≤ 0.001	$F_{4/14} = 83.3$
	CLAVATA 3-like	≤ 0.001	$F_{4/14} = 48.1$
	ERIK	≤ 0.001	$F_{4/14} = 2516$
	Serotonin receptor	≤ 0.001	$F_{4/14} = 123.6$
	Salt tolerance-like	≤ 0.001	$F_{4/14} = 240.7$
	IAMT1-like	≤ 0.001	$F_{4/14} = 54.3$
	P450 82C4-like	≤ 0.001	$F_{4/14} = 17.2$
	Auxin induced 5NG4-like	≤ 0.001	$F_{4/14} = 60.9$
	Expansin	≤ 0.001	$F_{4/14} = 28.2$
	Trichome birefringence-like 27	≤ 0.001	$F_{4/14} = 20.4$
	NBS-LRR	≤ 0.001	$F_{4/14} = 80.1$
	Basic-leucine zipper TF	≤ 0.001	$F_{4/14} = 515.6$
	Somatic-embryogenesis RLK1	≤ 0.01	$F_{4/14} = 5.42$
	RLK	≤ 0.001	$F_{4/14} = 31.9$
Fig S17B	PR length	≤ 0.001	$F_{2/155} = 126.3$
	PER number	≤ 0.05	$F_{2/155} = 3.68$
	PER density	≤ 0.001	$F_{2/155} = 26.3$
Fig S17D	-	≤ 0.001	$F_{2/16} = 11.3$
Fig S17E	-	≤ 0.01	$F_{2/15} = 11$
Fig S18B	PR length	≤ 0.001	$F_{5/276} = 100.6$
	PER number	≤ 0.001	$F_{5/276} = 25$
	PER density	≤ 0.001	$F_{5/276} = 52.8$
Fig S18D	-	≤ 0.001	$F_{5/42} = 17.1$
Fig S18E	-	≤ 0.001	$F_{5/42} = 59.1$
Fig S19B	WT	≤ 0.001	$F_{3/156} = 562.8$
	smax1-2	≤ 0.001	$F_{3/156} = 371.1$
	smax1-3	≤ 0.001	$F_{3/156} = 166.4$
Fig S19B	Mock (Dunnett's test)	≤ 0.001	$F_{2/117} = 462.2$
Fig S19C	WT	≤ 0.001	$F_{3/156} = 91.3$
	smax1-2	≤ 0.001	$F_{3/156} = 37.8$

	smax1-3	≤ 0.05	$F_{3/156} = 3.76$
Fig S19C	Mock (Dunnett's test)	= 0.578	$F_{2/117} = 0.55$
Fig S19D	-	≤ 0.001	$F_{5/174} = 104.8$
Fig S19E	-	≤ 0.001	$F_{5/174} = 104.8$
Fig S19F	Dark grown	≤ 0.01	$F_{2/6} = 18$
	Light grown	≤ 0.05	$F_{2/6} = 9.57$
Fig S20A	*Germin-like*	≤ 0.001	$F_{5/12} = 11.5$
	IAMT1-like	≤ 0.001	$F_{5/12} = 18.8$
	Auxin-induced 5NG4-like	≤ 0.001	$F_{5/12} = 27.9$
	Expansin	≤ 0.001	$F_{5/12} = 18.9$
	DLK2	≤ 0.001	$F_{5/12} = 148.3$
	ERIK	≤ 0.001	$F_{5/12} = 22.3$
	Unknown	≤ 0.001	$F_{5/12} = 57.6$
	Serotonin receptor	≤ 0.001	$F_{5/12} = 47.8$
Fig S20B	*Germin-like*	≤ 0.001	$F_{5/12} = 12.5$
	IAMT1-like	≤ 0.001	$F_{5/12} = 24.2$
	Auxin-induced 5NG4-like	≤ 0.001	$F_{5/12} = 20$
	Expansin	≤ 0.001	$F_{5/12} = 113.1$
	DLK2	≤ 0.001	$F_{5/12} = 283.8$
	ERIK	≤ 0.001	$F_{5/12} = 109.8$
	Unknown	≤ 0.001	$F_{5/12} = 49.3$
	Serotonin receptor	≤ 0.001	$F_{5/12} = 23.1$
Fig S21A	*DLK2*	≤ 0.001	$F_{5/18} = 137.6$
	ERIK	≤ 0.001	$F_{5/18} = 56.1$
	Unknown	≤ 0.05	$F_{5/18} = 4.17$
	Serotonin receptor	≤ 0.001	$F_{5/18} = 72.4$
	Germin-like	= 0.65	$F_{5/18} = 0.67$
Fig S21B	*DLK2*	≤ 0.001	$F_{3/12} = 104.2$
	ERIK	≤ 0.001	$F_{3/12} = 192$
	Serotonin receptor	≤ 0.01	$F_{3/12} = 9.54$
	Germin-like	= 0.13	$F_{3/12} = 2.32$
Fig S22A	-	≤ 0.01	$F_{5/18} = 6.1$
Fig S22B	-	≤ 0.001	$F_{3/12} = 27.43$
Fig S22C	-	= 0.11	$F_{3/31} = 2.18$
Fig S22D	PR length	≤ 0.001	$F_{3/236} = 164.9$
	PER number	≤ 0.001	$F_{3/236} = 116$
	PER density	≤ 0.001	$F_{3/236} = 101.1$
Fig S22E	PR length	≤ 0.001	$F_{3/164} = 149.4$
	PER number	≤ 0.001	$F_{3/164} = 96.6$
	PER density	≤ 0.001	$F_{3/164} = 144.9$
Fig S23E	-	≤ 0.001	$F_{9/88} = 97.4$

Table S8. Number of DEGs per genotype and number of genotype specific DEGs with reference to the wild type.

Genotype	Number of DEGs	Specific DEGs	Shared DEGs
kai2a-1 kai2b-1	1476	280 (19,0 %)	1196 (81,0 %)
max2-4	1720	511 (29,7 %)	1209 (70,3 %)
smax1-2	3113	471 (15,1 %)	2642 (84,9 %)
smax1-3	3818	971 (25,4 %)	2847 (74,6 %)

Table S9. Overlap of DEGs among genotypes.

Intersection	DEG overlap
smax1-2 ∩ *smax1-3*	2511 (56,8 %)
kai2a-1 kai2b-1 ∩ *max2-4*	765 (31,5 %)
kai2a-1 kai2b-1 ∩ *smax1-2*	872 (23,4 %)
kai2a-1 kai2b-1 ∩ *smax1-3*	988 (22,9 %)
max2-4 ∩ *smax1-3*	989 (21,7 %)
max2-4 ∩ *smax1-2*	848 (21,3 %)
All mutants	506 (9,5 %)

References

1. A. Malolepszy *et al.*, The *LORE1* insertion mutant resource. *Plant J* **88**, 306-317 (2016).
2. D. Reid *et al.*, Dynamics of ethylene production in response to compatible nod factor. *Plant Physiol* **176**, 1764-1772 (2018).
3. S. Carbonnel *et al.* (2019) Duplicated KAI2 receptors with divergent ligand-binding specificities control distinct developmental traits in *Lotus japonicus*. (BioRxiv 754937).
4. M. T. Waters *et al.*, Specialisation within the DWARF14 protein family confers distinct responses to karrikins and strigolactones in Arabidopsis. *Development* **139**, 1285-1295 (2012).
5. J. P. Stanga, S. M. Smith, W. R. Briggs, D. C. Nelson, *SUPPRESSOR OF MORE AXILLARY GROWTH2 1* controls seed germination and seedling development in Arabidopsis. *Plant Physiol* **163**, 318-330 (2013).
6. S. Huang *et al.*, A type III ACC synthase, ACS7, is involved in root gravitropism in *Arabidopsis thaliana*. *J Exp Bot* **64**, 4343-4360 (2013).
7. P. Guzmán, J. R. Ecker, Exploiting the triple response of Arabidopsis to identify ethylene-related mutants. *Plant Cell* **2**, 513-523 (1990).
8. J. A. Villaecija-Aguilar *et al.*, SMAX1/SMXL2 regulate root and root hair development downstream of KAI2-mediated signalling in Arabidopsis. *PLoS Genet* **15**, e1008327 (2019).

9. M. Maekawa-Yoshikawa *et al.*, The temperature-sensitive *brush* mutant of the legume *Lotus japonicus* reveals a link between root development and nodule infection by rhizobia. *Plant Physiol* **149**, 1785-1796 (2009).
10. K. Yano *et al.*, CYCLOPS, a mediator of symbiotic intracellular accommodation. *Proc Natl Acad Sci U S A* **105**, 20540-20545 (2008).
11. A. Binder *et al.*, A modular plasmid assembly kit for multigene expression, gene silencing and silencing rescue in plants. *PLoS One* **9**, 1-14 (2014).
12. J. Trifinopoulos, L. Nguyen, A. von Haeseler, B. Q. Minh, W-IQ-TREE: a fast online phylogenetic tool for maximum likelihood analysis. *Nucleic Acids Res* **44**, W232-W235 (2016).
13. S. Kumar, G. Stecher, M. Li, C. Knyaz, K. Tamura, MEGA X: Molecular Evolutionary Genetics Analysis across computing platforms. *Mol Biol Evol* **35**, 1547-1549 (2018).
14. T. Czechowski, R. P. Bari, M. Stitt, W. Scheible, M. K. Udvardi, Real-time RT-PCR profiling of over 1400 Arabidopsis transcription factors: unprecedented sensitivity reveals novel root- and shoot-specific genes. *Plant J* **38**, 366-379 (2004).
15. R. Patro, G. Duggal, M. I. Love, R. A. Irizarry, C. Kingsford, Salmon provides fast and bias-aware quantification of transcript expression. *Nat Methods* **14**, 417-419 (2017).
16. T. Mun, A. Bachmann, V. Gupta, J. Stougaard, S. U. Andersen, Lotus Base: An integrated information portal for the model legume *Lotus japonicus*. *Sci Rep* **6**, 1-18 (2016).
17. C. Soneson, M. I. Love, M. D. Robinson, Differential analyses for RNA-seq: transcript-level estimates improve gene-level inferences. *F1000Res* **4**, 1-18 (2015).
18. Z. Du, X. Zhou, Y. Ling, Z. Zhang, Z. Su, agriGO: a GO analysis toolkit for the agricultural community. *Nucleic Acids Res* **38**, W64-70 (2010).
19. J. P. Stanga, N. Morffy, D. C. Nelson, Functional redundancy in the control of seedling growth by the karrikin signaling pathway. *Planta* **243**, 1397-1406 (2016).
20. G. Sun *et al.*, N-terminus-mediated degradation of ACS7 is negatively regulated by senescence signaling to allow optimal ethylene production during leaf development in Arabidopsis. *Front Plant Sci* **8**, 2066 (2017).
21. L. Xiong, D. Xiao, X. Xu, Z. Guo, N. N. Wang, The non-catalytic N-terminal domain of ACS7 is involved in the post-translational regulation of this gene in Arabidopsis. *J Exp Bot* **65**, 4397-4408 (2014).

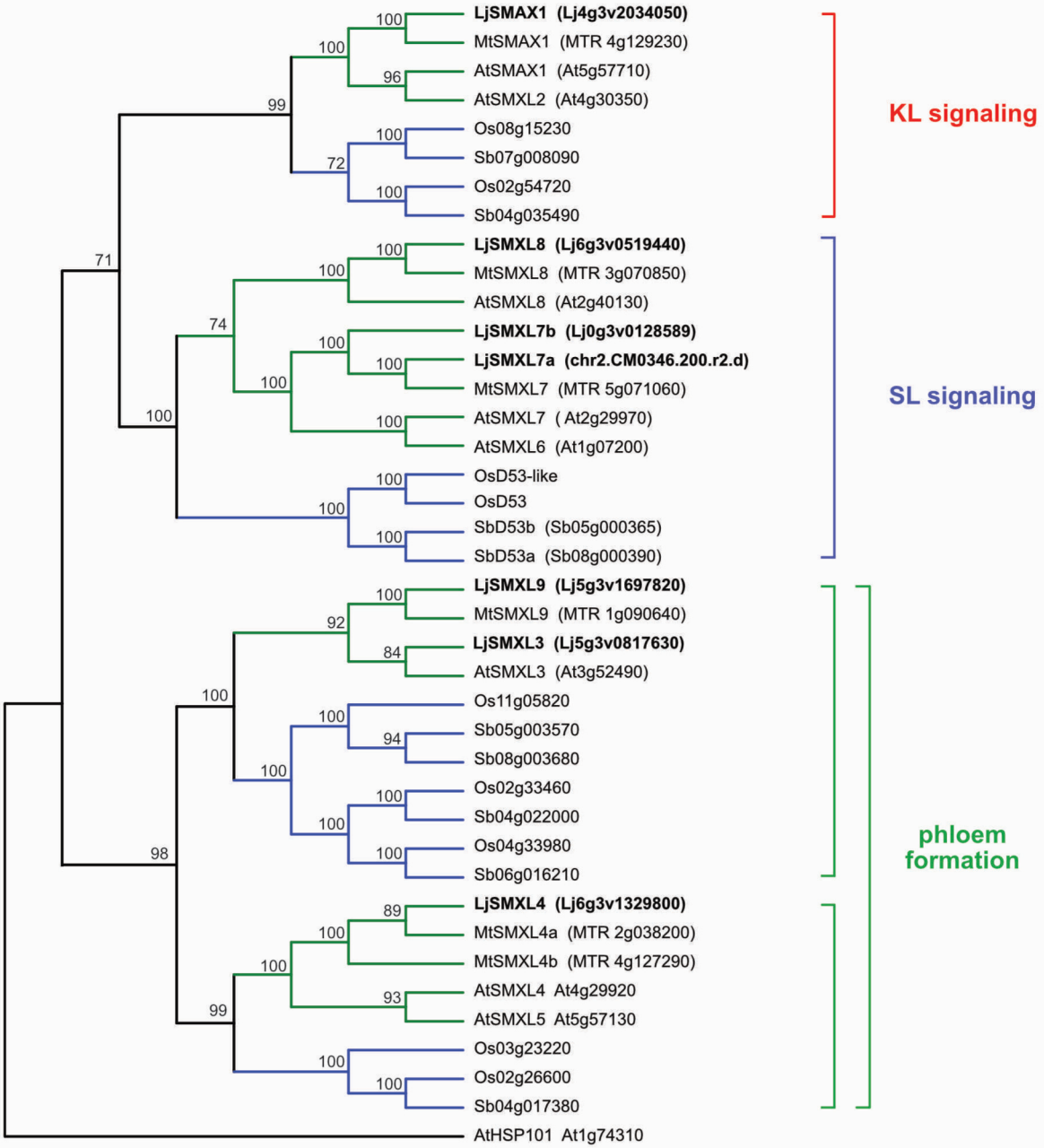

Fig. S1. SMAX1 is a single copy gene in *L. japonicus.* Phylogenetic tree of SMAX1 and SMXL proteins from *L. japonicus, Arabidopsis thaliana, Medicago truncatula, Sorghum bicolor,* and *Oryza sativa*, rooted with AtHSP101. Branch colors indicate monocotyledons (blue) and dicotyledons (green). Bootstrap values of 1000 repetitions are indicated at each node. The four SMXL clades are indicated by a colored bracket and their described function.

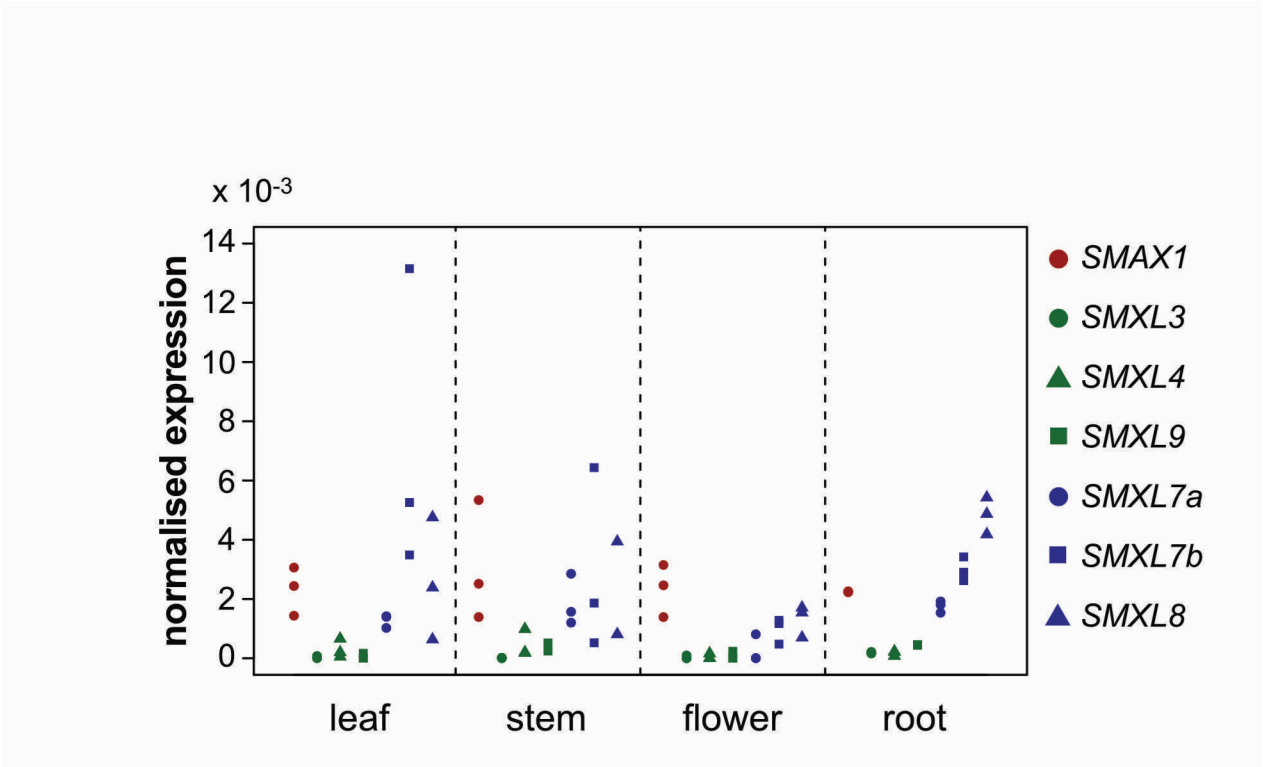

Fig. S2. Transcript accumulation of *L. japonicus SMXL* genes in different plant organs. Transcript accumulation was determined by RT-qPCR using cDNA from *L. japonicus* plants grown in pots (n = 3). Colors indicate described involvement of the genes in known signaling pathways or developmental processes: KAR/KL signaling (red), phloem formation (green), and SL signaling (blue).

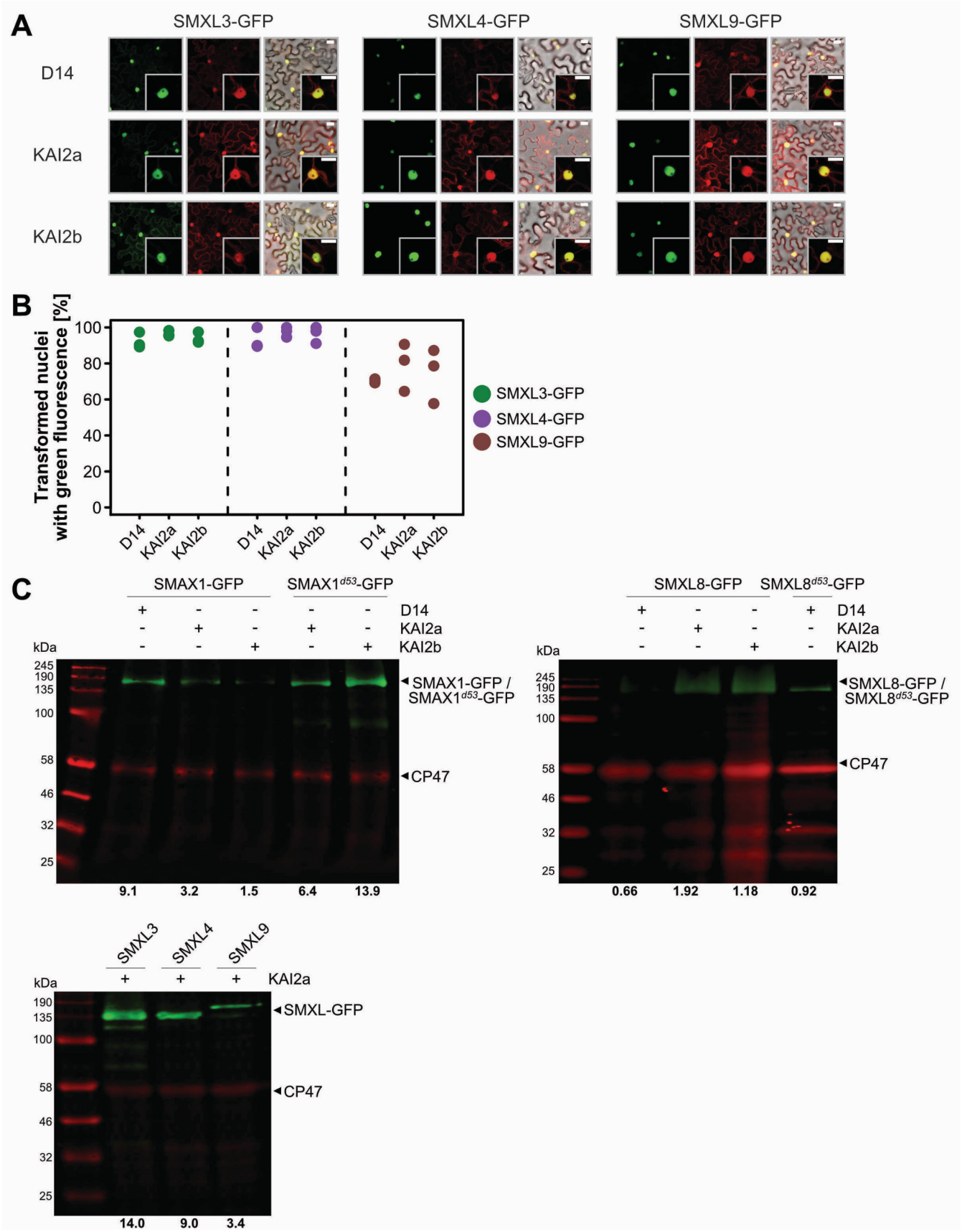

Fig. S3. (A) SMXL3, 4, and 9 are not degraded in presence of D14, KAI2a or KAI2b, and MAX2. Confocal microscopy images of *N. benthamiana* leaves expressing the indicated SMXLs fused with GFP, a free mCherry transformation marker, and any of the α/β-hydrolase receptors HA-D14, HA-KAI2a, or HA-KAI2b. For each combination, green fluorescence of SMXL-GFP fusions is shown on the left, red-fluorescence of the mCherry transformation marker in the middle, and an overlay of green and red fluorescence and bright-field images on the right. All proteins were encoded on the same plasmid (see Fig. 1A). Insets at the bottom-right corner show a single nucleus at higher magnification. Scale bars = 25µm. **(B)** Percentage of green fluorescent nuclei (indicating presence of SMXLs) per red fluorescent nuclei (indicating successful transformation) in microscopic images of leaf epidermal cells of *N. benthamiana* in presence of the HA-tagged α/β-fold hydrolase receptor indicated at the x-axis and presence of MYC-MAX2. In each image 21 to 97 nuclei were analyzed, n = 3 images per protein combination. **(C)** Anti-GFP immunoblot of protein extracts from *N. benthamiana* leaf disks expressing the indicated *L. japonicus* SMXLs and alpha-beta hydrolase receptors as well as MAX2. The autofluorescent photosystem II P680 chlorophyll A apoprotein, CP47 (PsbB, predicted MW 56.6 kD) was used as loading control. Numbers below the lanes indicate the ratio of fluorescence signal intensities of the green fluorescent SMXL-GFP bands vs. the corresponding red fluorescent CP47 bands.

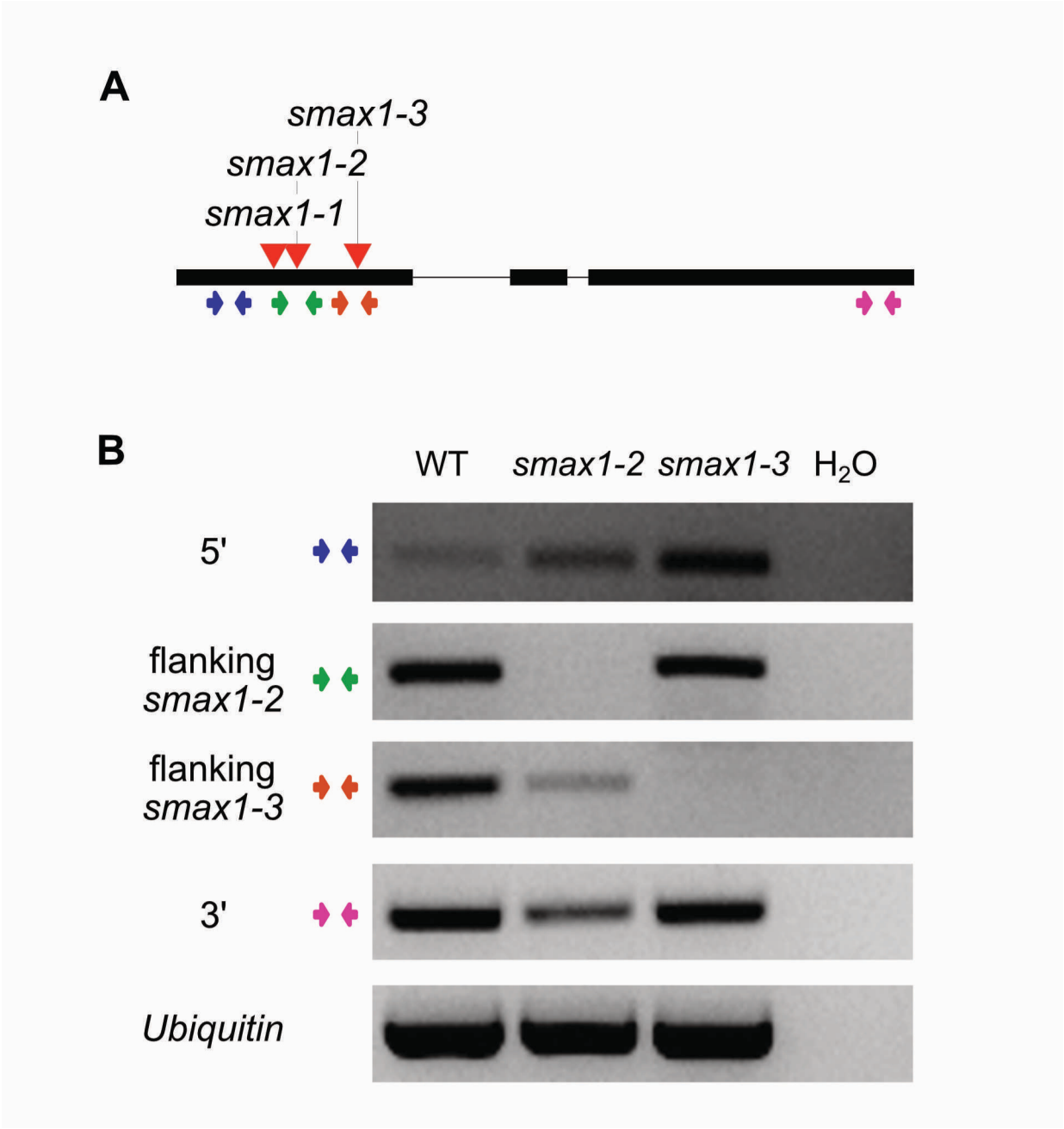

Fig. S4. Description of *smax1* LORE1 insertion mutants. **(A)** Schematic representation of the *L. japonicus SMAX1* gene. Black boxes and lines show exons and introns, respectively. *LORE1* insertions are indicated by red triangles, labeled with the number of the respective mutant allele. **(B)** *LjSMAX1* transcript accumulation in wild type, *smax1-2* and *smax1-3* mutants by RT-PCR using primer pairs located at the 5' (blue) and 3' (pink) end of the gene, as well as flanking the *LORE1* insertions of *smax1-2* (green) and *smax1-3* (orange). Positions of primer pairs are indicated in **(A)**. Transcript accumulation of the housekeeping gene *Ubiquitin* and a water control are also shown.

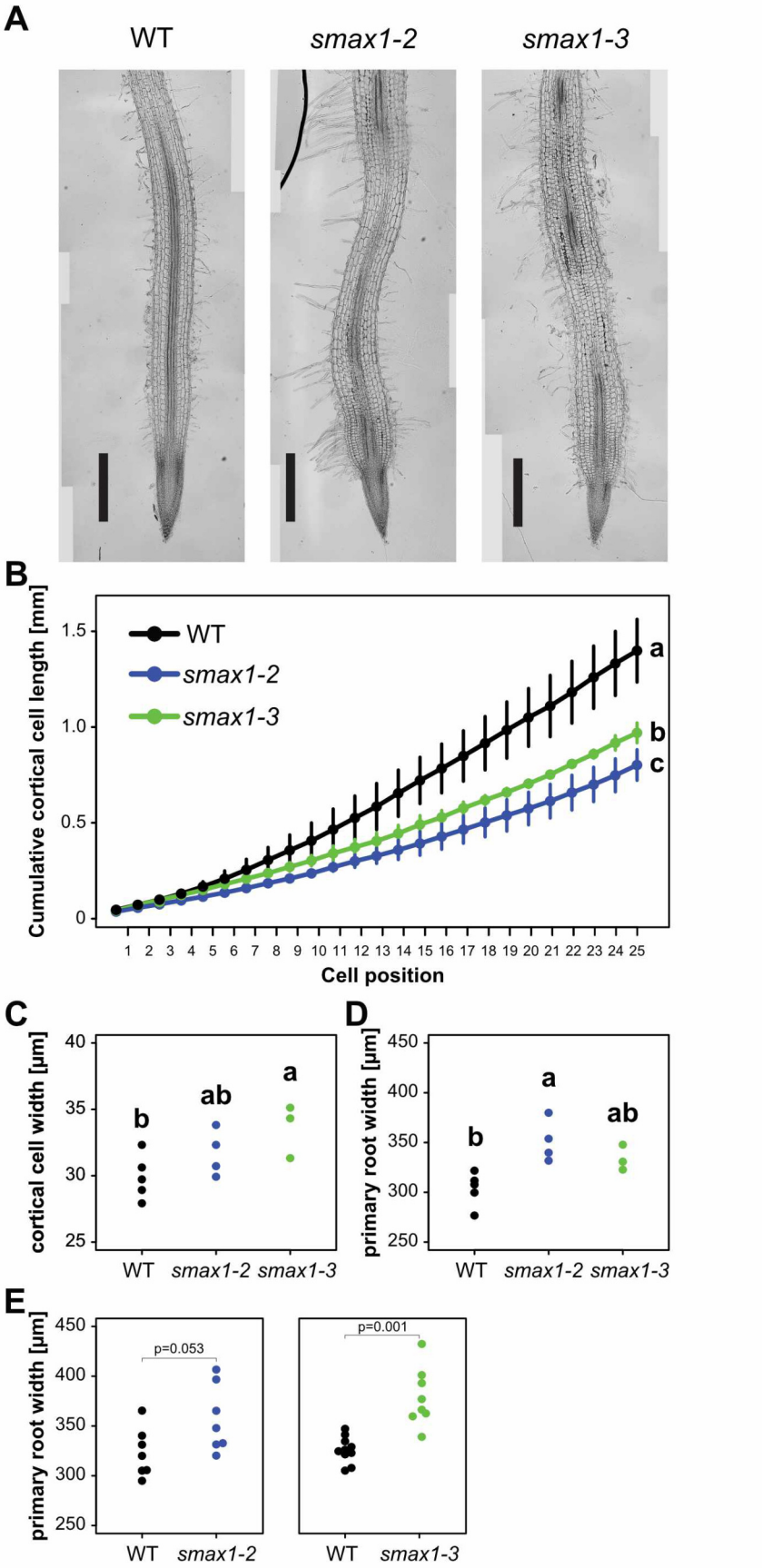

Fig. S5. Cortex cell elongation is perturbed in *smax1* mutants. **(A)** Representative images of longitudinal sections of primary roots of wild type, *smax1-2* and *smax1-3*. Scale bar = 500µm. **(B)** Cumulative length of 25 external cortical cells starting from the first observable cortical cell in the meristematic zone (n ≥ 3). **(C)** Width of cortical cells between 1 and 5 mm from the tip (n ≥ 3). **(D-E)** Width of intact primary roots between 1 and 10 mm from the tip (**(D)** n ≥ 3; **(E)** n ≥ 7). **(B-D)** Letters indicate significant differences (**(C)** two-way ANOVA; **(C-D)** one-way ANOVA, post-hoc Tukey test). **(E)** Asterisks indicate significant differences compared to the wild type (Welch t-test).

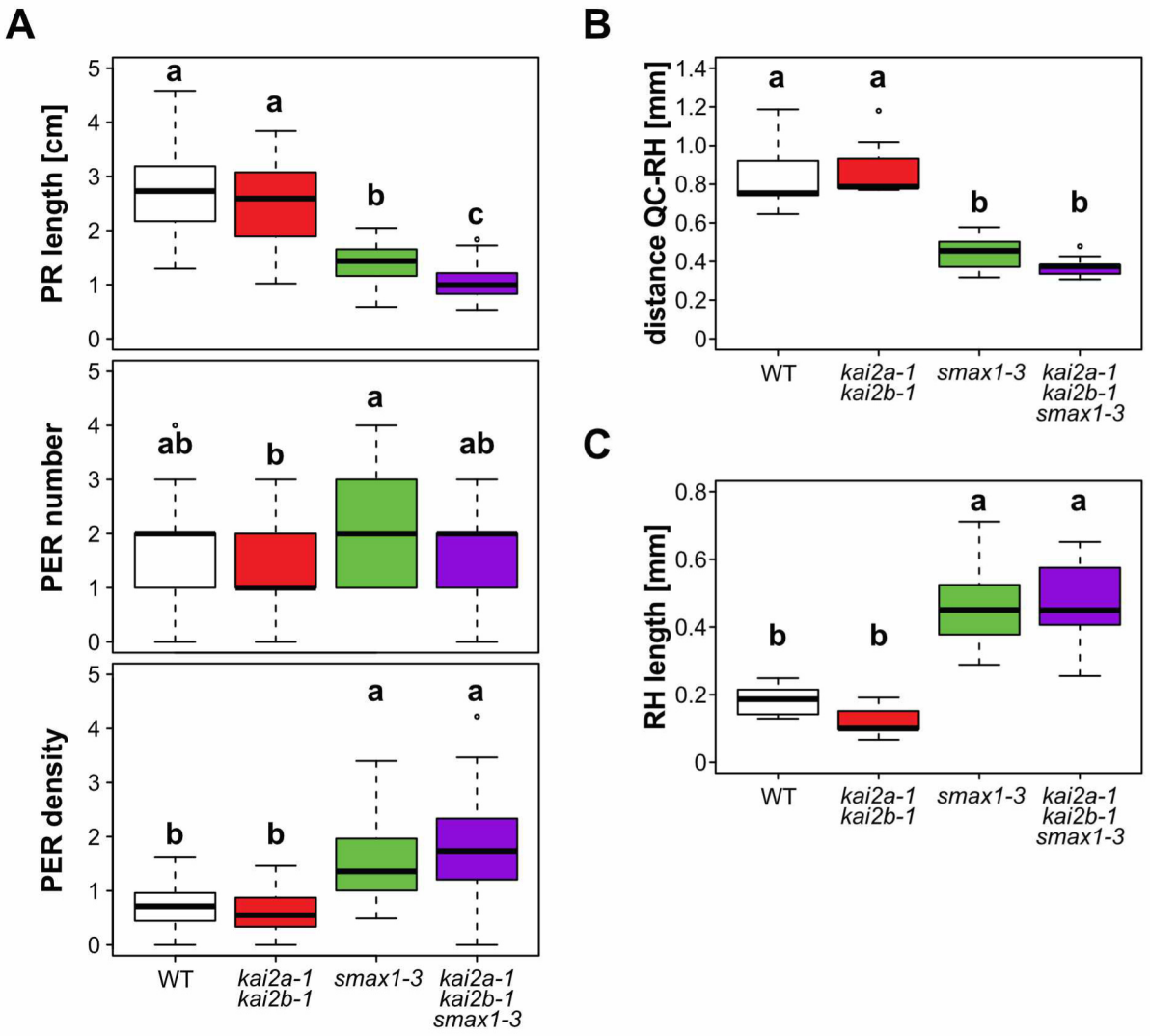

Fig. S6. *smax1* is epistatic to *kai2a kai2b*. **(A)** Primary root (PR) length, post-embryonic root (PER) number, and PER density of 10-day-old seedlings of the indicated genotypes (n ≥ 37). **(B)** Distance between the first root-hair (RH) and the quiescent-center (QC), and **(C)** the RH length of the indicated genotypes (n = 9). **(A, B, C)** Letters indicate significant differences (ANOVA, post-hoc Tukey test).

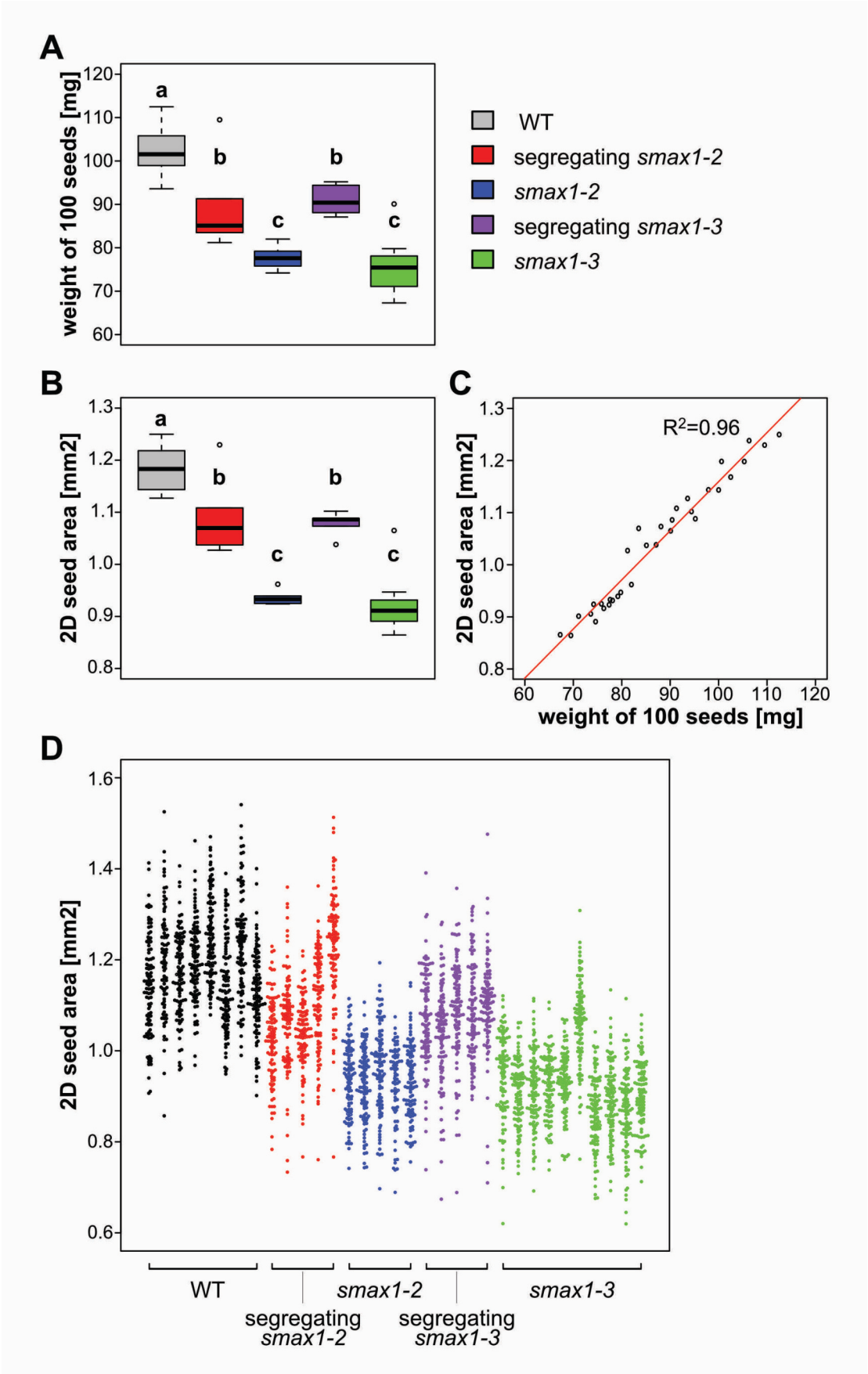

Fig. S7. *smax1* mutants produce smaller seeds. **(A)** Weight of 100 seeds of the wild type, *smax1-2*, *smax1-3*, and of populations segregating the *smax1-2* or *smax1-3* LORE1 insertion (n ≥ 5). **(B)** 2D area of the same seeds shown in **(A)** after high-resolution scanning. **(C)** Linear regression of the seed weight and 2D area. **(D)** Single 2D seed area of several seed populations (n ≥ 5). **(A-C)** Letters indicate significant differences (ANOVA, post-hoc Tukey test).

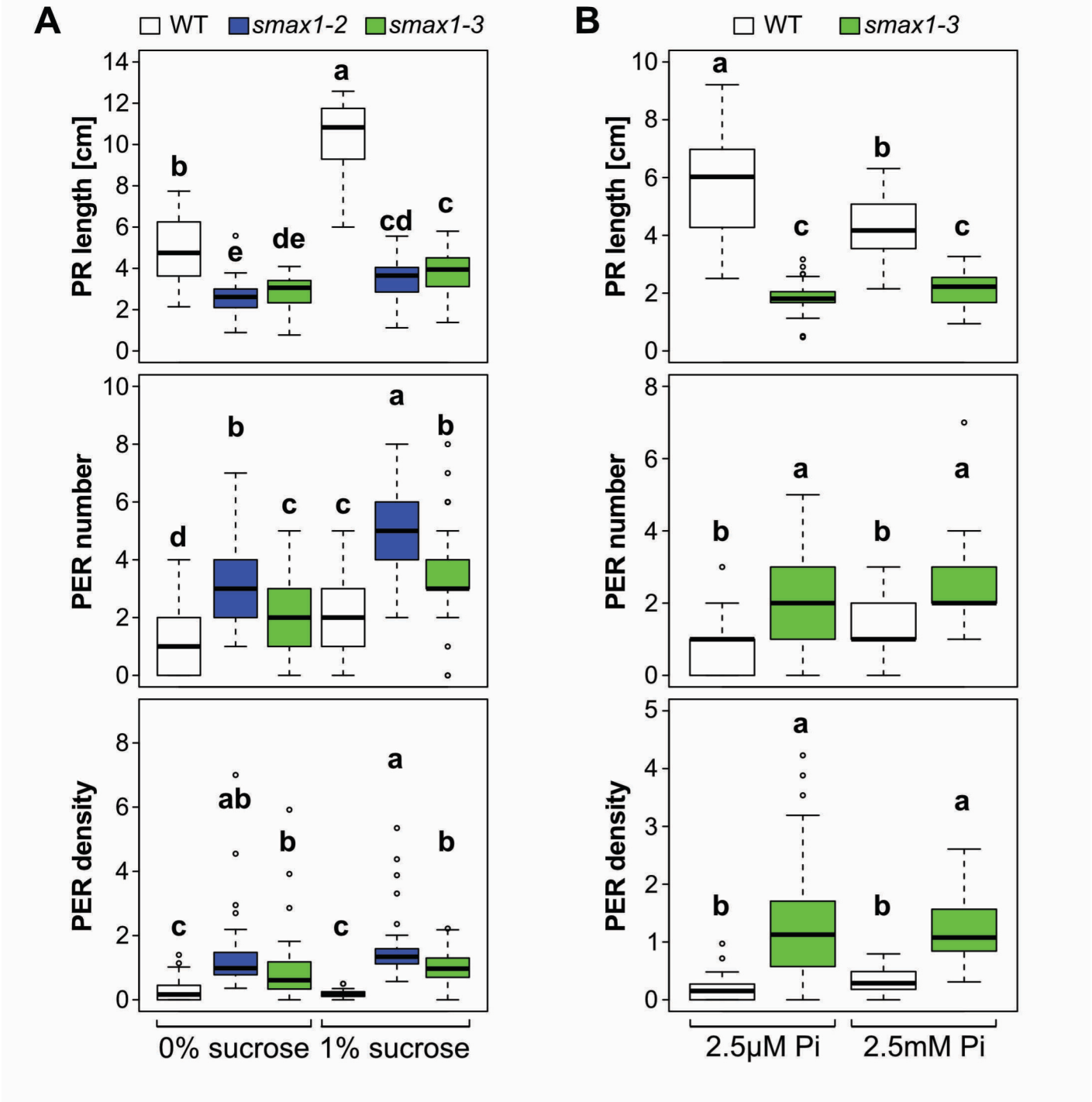

Fig. S8. Increased phosphate and sucrose availability does not rescue the short primary root of *smax1* mutants. **(A)** Primary root (PR) length, post-embryonic root (PER) number, and PER density of the indicated genotypes at 10 days post-germination grown **(A)** without or with 1 % sucrose (n ≥ 43), and **(B)** with 2.5µM (Low Pi) or 2.5mM (High Pi) phosphate (n ≥ 28). Letters indicate significant differences (ANOVA, post-hoc Tukey test).

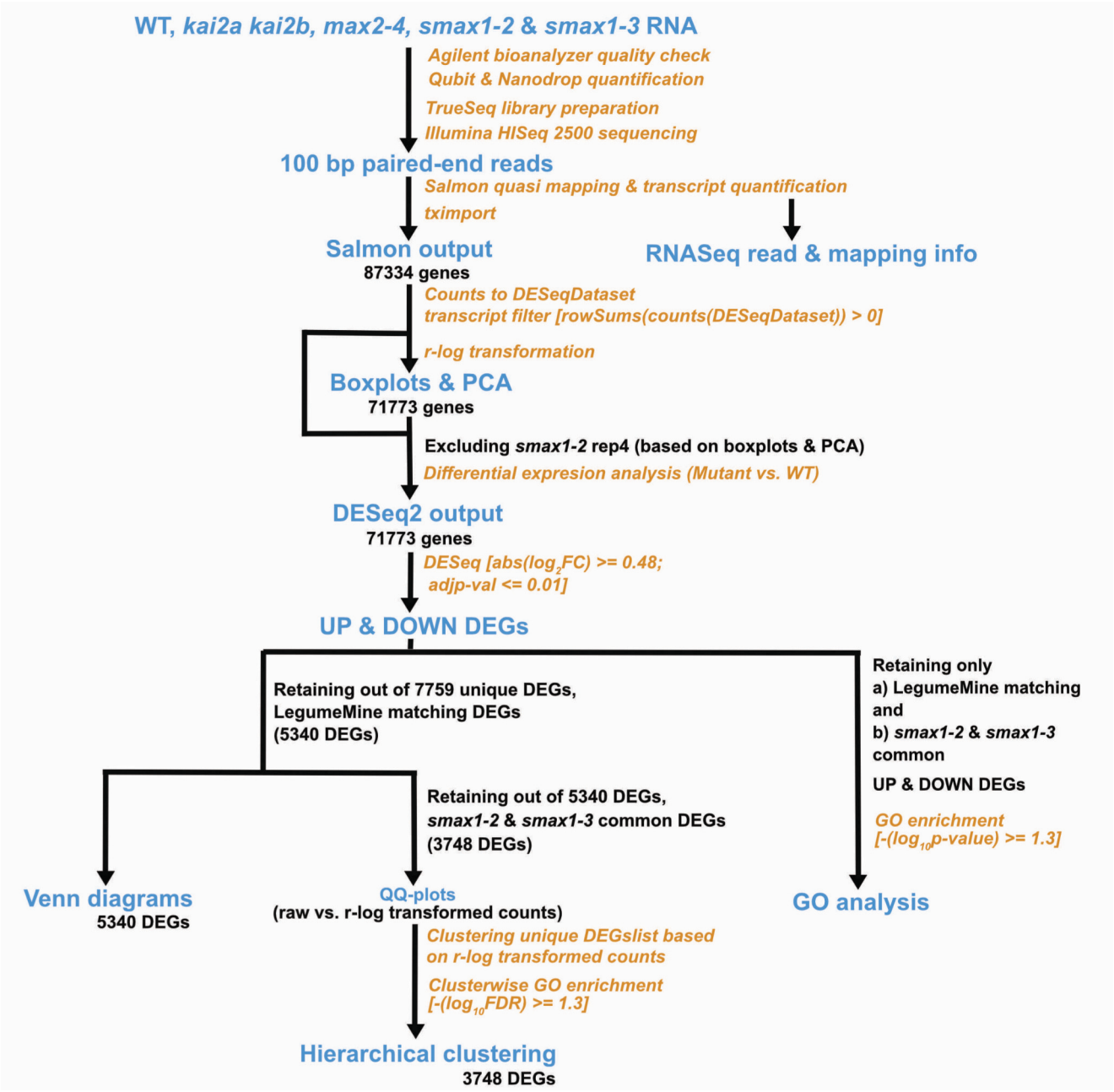

Fig. S9. RNA sequencing data analysis pipeline**.** Blue color indicates figures and datasets. Orange color indicates operations and functions utilized in the analyses. Total RNA isolated from the different genotypes was checked for quality on an Agilent Bioanalyzer and quantified with Qubit. High quality total RNA was processed with the TruSeq Stranded kit (Illumina) for library preparation and then fragments were sequenced on an Illumina HiSeq 2500 to obtain "100 bp paired end reads". The reads were quality checked with fastqc() in Conda (in BASH, Windows Linux subsystem). The reads were mapped to the reference transcriptome (Lotusjaponicus_MG20_v3.0_cdna.fa, downloaded from *Lotus* Base, (16) using the Salmon quasi mapping approach (15), followed by transcript quantification at gene level for 87334 genes in conda (in BASH). "RNASeq read and mapping info" was obtained for each sample alongside quantification. Subsequently, tximport() in R (17) was used for extracting raw read count, transcript length and TPM counts for 87334 genes in a single matrix table "Salmon output". From Salmon output, only 71773 genes were retained after removing genes with 0 reads in all the samples using DESeq dataset transcript filter. DESeq package in Bioconductor was used for a) data exploration using sample "Boxplots and PCA" followed by differential expression analysis ("DESeq2 output"), while excluding *smax1-2* replicate 4 (based on read and mapping info and PCA). "UP & DOWN DEGs" describing upregulated and downregulated genes in each mutant vs. wild type comparison were obtained from DESeq2 output using a cut-off of logFC ≥ |0.48| and adjp-val ≤ 0.01. 7759 unique DEGs were obtained by combining all these DEGs from the four mutants vs. wild type comparisons. Out of these, LegumeMine identified 5340 DEGs, which were further used for preparing "Venn diagrams" between DEGs of mutant vs. wild type comparisons. The r-log transformed read data were used for "Hierarchical clustering" of 3748 DEGs (obtained by excluding the DEGs from the group of 5340 DEGs, which were unique to only one of the *smax1* mutants). Diagnostic plots assessing use of raw counts and r-log transformed counts for suitability in hierarchical clustering are provided in "QQ-plots". Gene-ontology enrichment analysis (cut-off $-\log_{10}$FDR ≥ 1.3) with AgriGO (18) was used to find over-represented biological processes in each of the clusters obtained in "Hierarchical clustering". Another "GO comparison" was performed for UP & DOWN DEGs of *kai2a kai2b*, *max2-4,* and DEGs common to *smax1-2* and *smax1-3* (referred to as *smax1*). $-\log_{10}$FDR values for this comparison were displayed as heatmap for enriched biological terms.

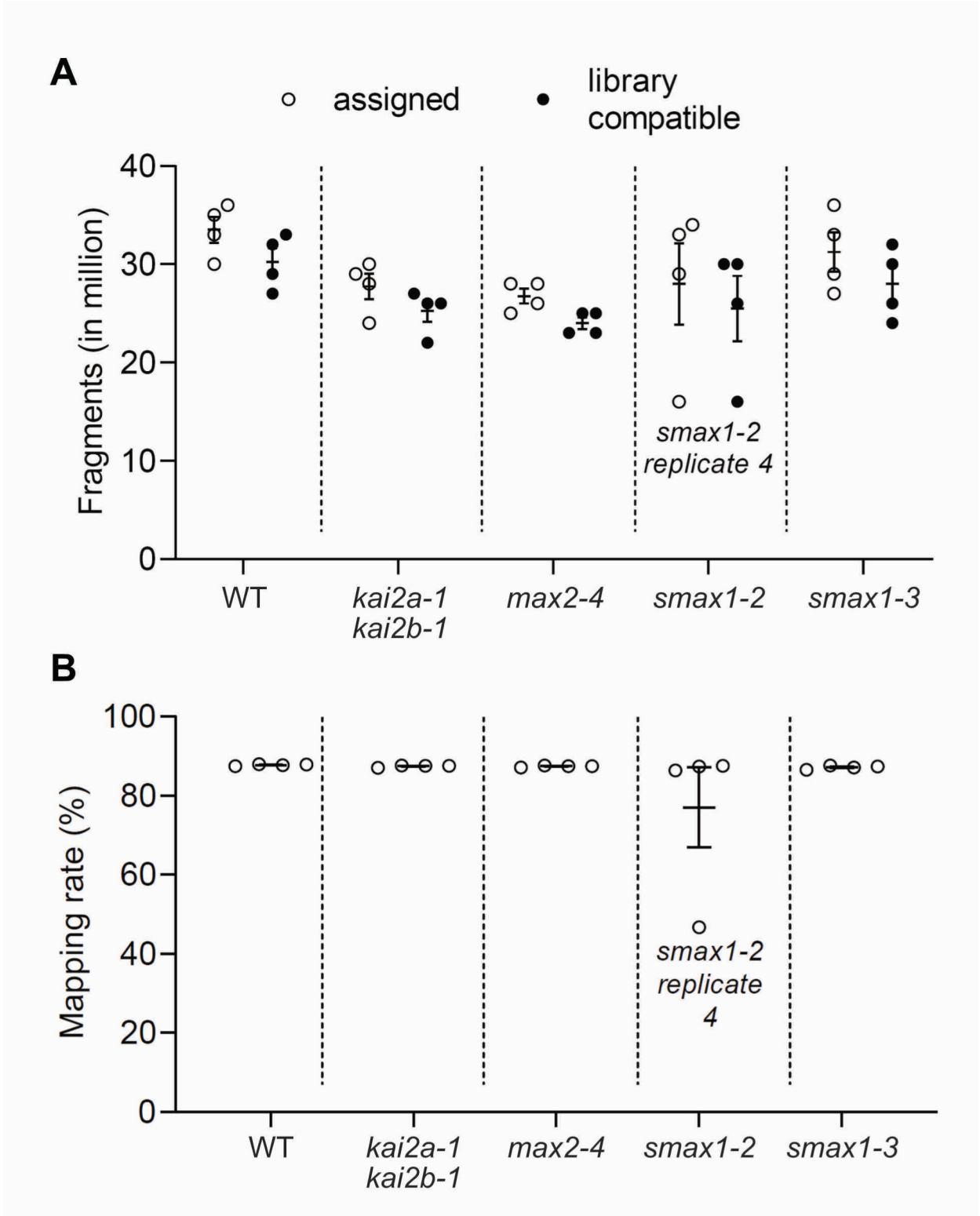

Fig. S10. Number of reads and mapping rate for the RNA sequencing data. **(A)** Number of reads obtained for the sequencing data along with the number of reads matching the Inverted Stranded Reverse (ISR) library used (https://salmon.readthedocs.io/en/latest/library_type.html). **(B)** Percentage of reads mapping to the reference transcriptome (Lotusjaponicus_MG20_v3.0_cdna.fa, downloaded from LotusBase) used in the salmon operation. Replicate 4 of *smax1-2* was removed from further analysis, since it suffered from incompatible library reads.

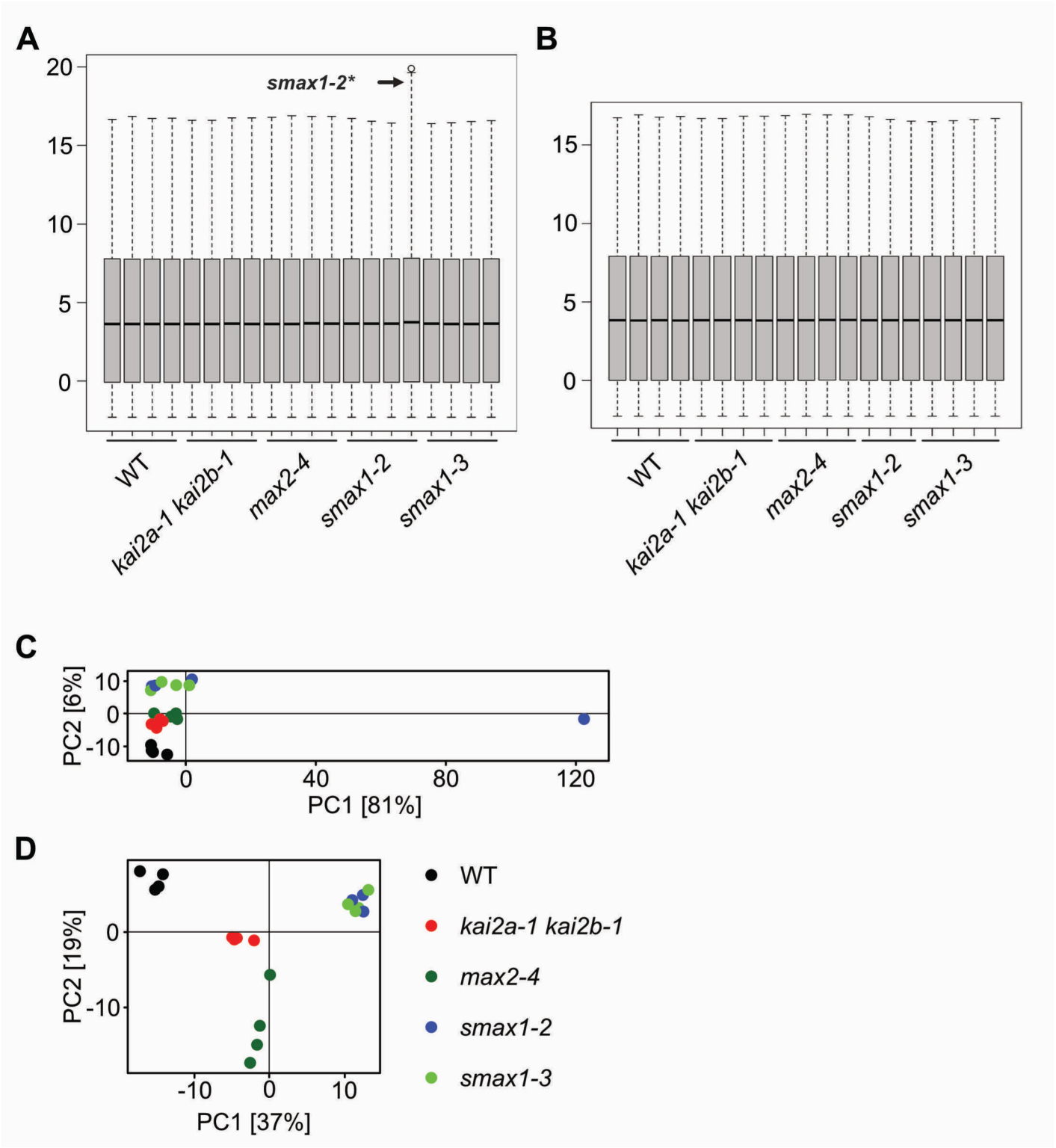

Fig. S11. Sample boxplots and PCA plots for preliminary data exploration. **(A-B)** Overall density distributions of r-log transformed count data variation among samples. **(C-D)** The rlog transformed count data were projected onto the first two principal components. The expected variation between wild type, *kai2a-1 kai2b-1, max2-4,* and *smax1* mutants is clearly visible along PC1. Graphs **(A,C)** include all 20 samples while graphs **(B,D)** exclude *smax1-2**(replicate 4).

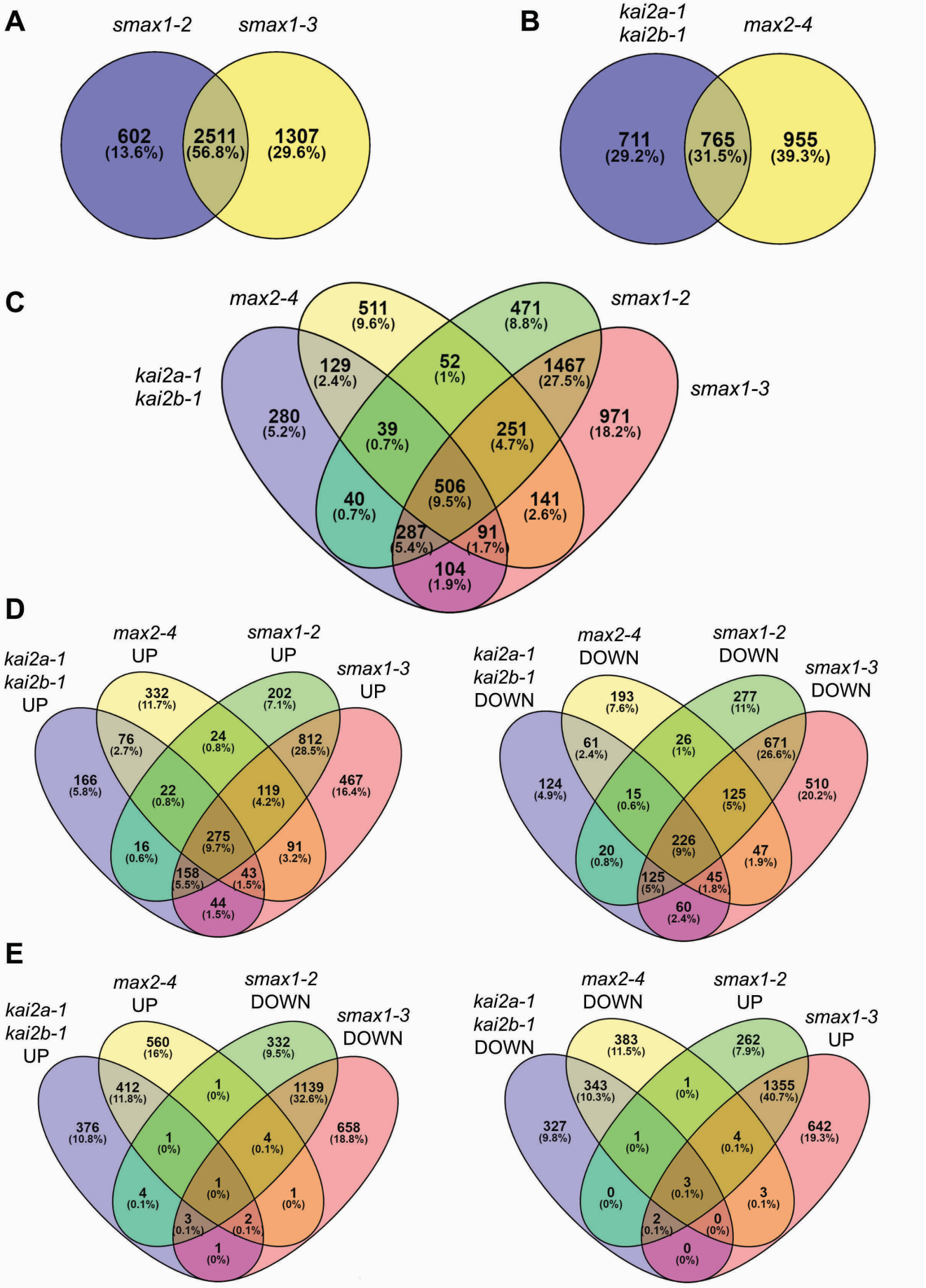

Fig. S12. Venn diagrams representing the overlap of the 5340 unique DEGs among karrikin signaling mutants. Overlap of DEGs (each mutant vs. wild type) between **(A)** *smax1-2* and *smax1-3* **(B)** *kai2a-1 kai2b-1* and *max2-4* **(C)** all four mutants. **(D)** Overlap among all four mutants of upregulated (left) and downregulated (right) DEGs. **(E)** Overlap of DEGs, which are regulated in opposite direction in *kai2a-1 kai2b-1* and *max2-4* vs. *smax1-2* and *smax1-3*. Percentage numbers represent the fraction of DEGs with respect to the total number of unique DEGs in the genotypes indicated in one Venn diagram.

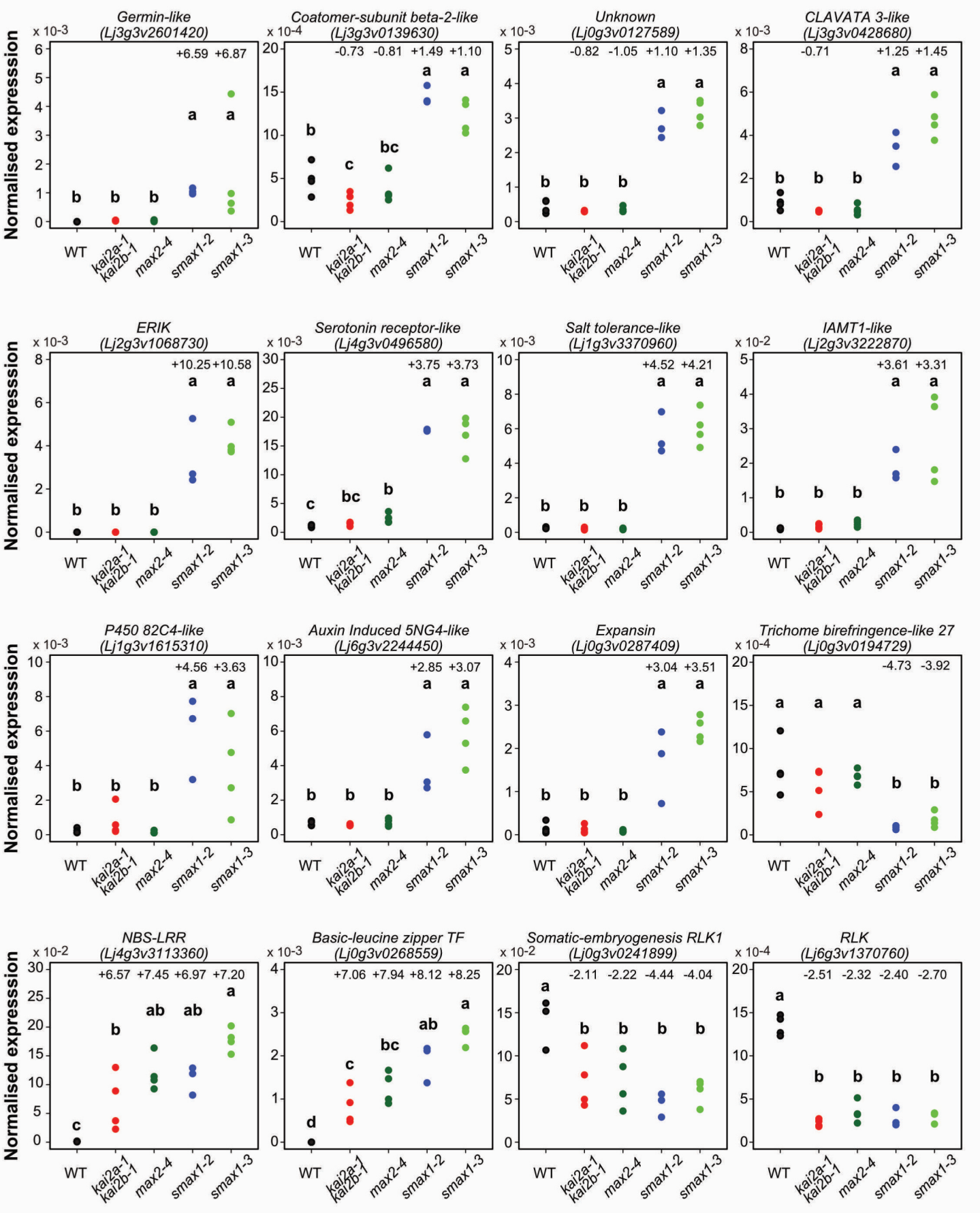

Fig. S13. qPCR-based transcript accumulation of selected DEGs recapitulates the RNAseq results. Expression values of indicated genes in roots of indicated genotypes were normalized to the expression of *Ubiquitin*. Letters indicate statistical differences between genotypes (ANOVA, post-hoc Tukey test, (n = 3-4). Numbers above the data points indicate, if significant, the log2 fold-change outcome of the RNAseq analysis of each mutant compared to the wild type.

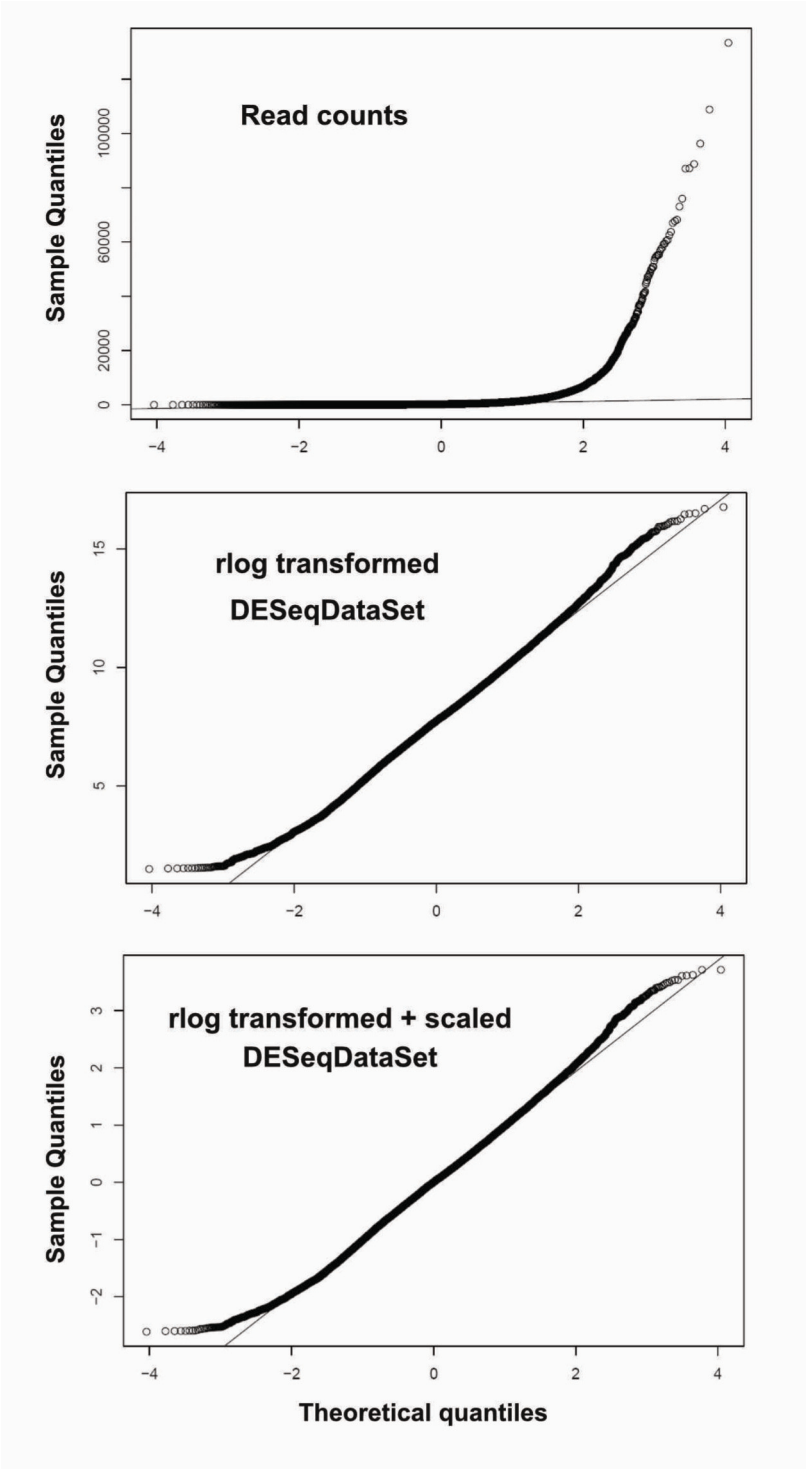

Fig. S14. QQ-plot for transcriptome data. Raw read count, r-log transformed counts, and scaled r-log transformed counts were used for scatter-plotting quantiles from our data vs. theoretical quantiles. Distribution suggests r-log transformation yields normally distributed data and makes them suitable for input into clustering algorithms.

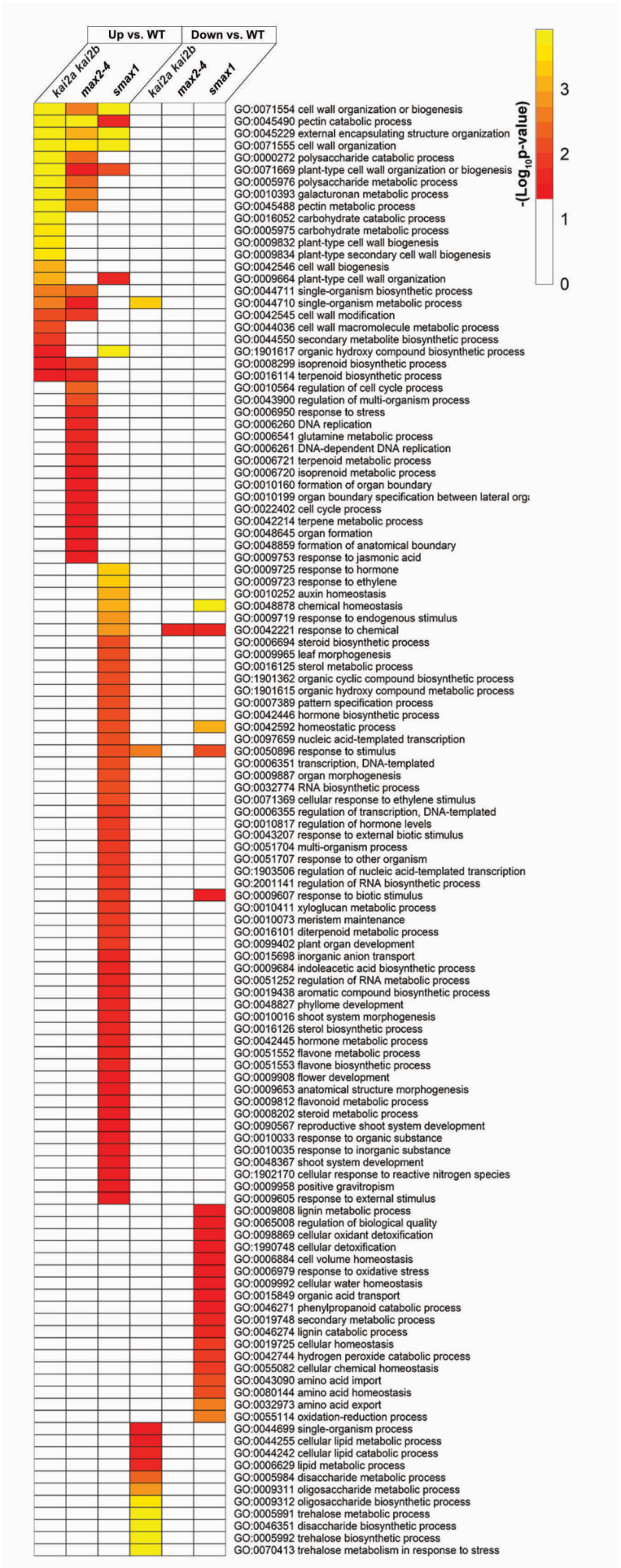

Fig. S15. Gene ontology (GO) enrichment analysis for DEGs of each mutant. GO enrichment analysis was performed using AgriGO for the up- and down-regulated genes in the mutant vs. wild type comparisons. $-\log_{10}$FDR ≥ 1.3 was used as cut-off and scores were represented by heatmap colors from red to yellow. White color indicates absence of statistical significance.

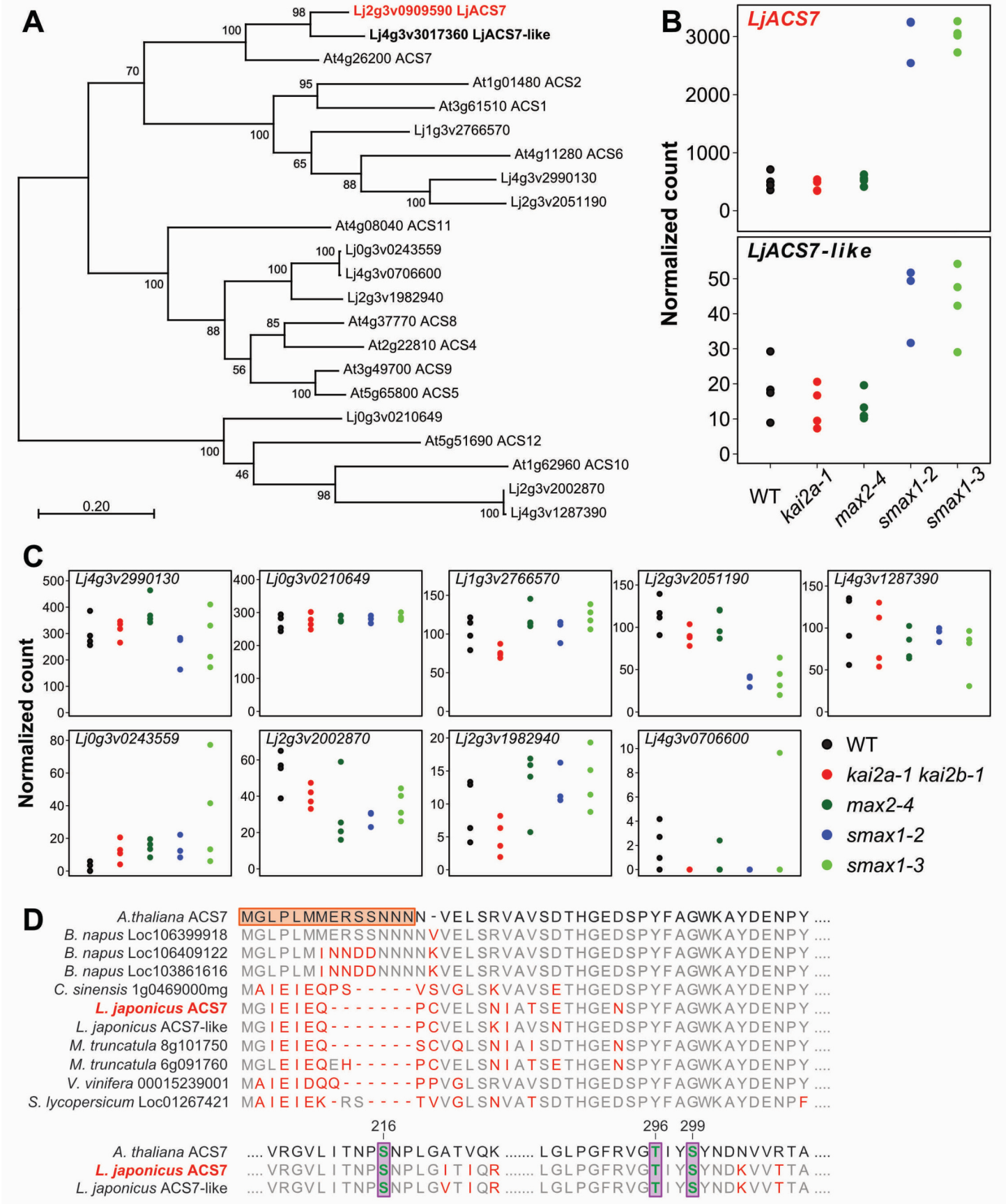

Fig. S16. *L. japonicus ACS7* is strongly expressed in *smax1* roots. **(A)** Phylogenetic tree of ACC-SYNTHASE (ACS) proteins from *A. thaliana* and *L. japonicus*. Protein sequences were aligned using MAFFT. MEGAX was used to generate a tree inferred by Maximum Likelihood method. The tree with highest log likelihood (-12384.37) is shown. The percentage of trees in which associated taxa clustered together is shown next to the branches. **(B-C)** RNAseq-based TPM (Transcripts Per Million) count of indicated *ACS* genes in roots of the indicated genotypes. **(D)** Protein alignments of ACS7 homologs from *Brassica napus*, *Medicago truncatula*, *Citrus sinensis*, *Vitis vinifera* and *Solanum lycopersicum*. The orange frame indicates the sequence reported by Xiong et al. to promote protein instability (20, 21). Green residues in purple frames indicate conserved phosphosites preventing protein degradation (6).

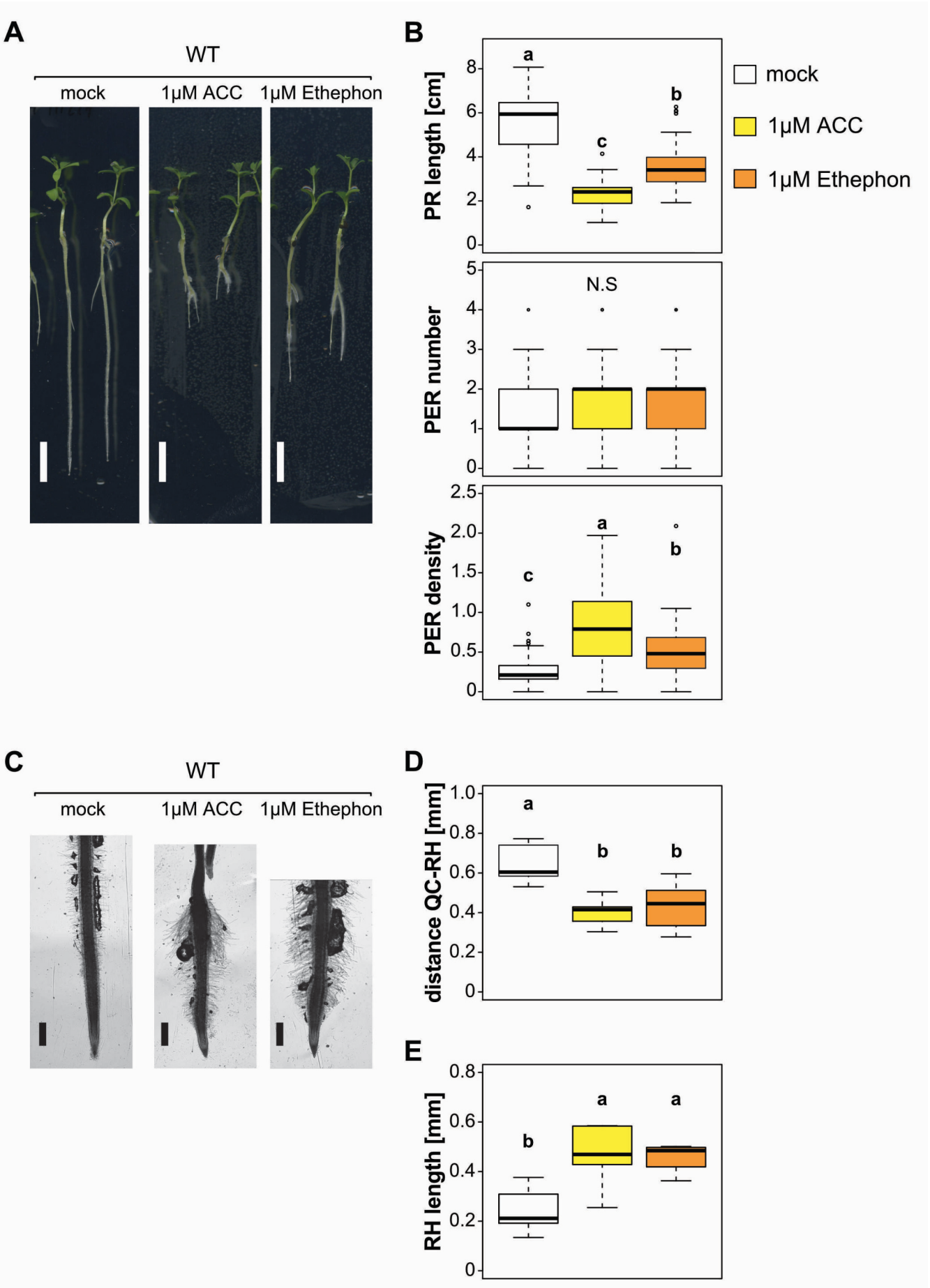

Fig. S17. Treatment with ethylene precursors causes *smax1*-like root and root-hair phenotypes in *L. japonicus* wild type. **(A)** Representative images (scale bar = 1cm) and **(B)** quantification of primary root (PR) length, post-embryonic root (PER) number, and PER density of 10-day-old wild type seedlings grown in presence of 1μM of ethylene precursor ACC and ethylene releasing chemical Ethephon (n ≥ 44). **(C)** Representative images of the root tip (scale bar = 500μm), **(D)** distance between the first root-hair (RH) and the quiescent-center (QC), **(E)** and the RH length of wild type seedlings grown in presence of 1μM ACC or Ethephon (n ≥ 4). **(B, D, E)** Letters indicate significant differences (ANOVA, post-hoc Tukey test).

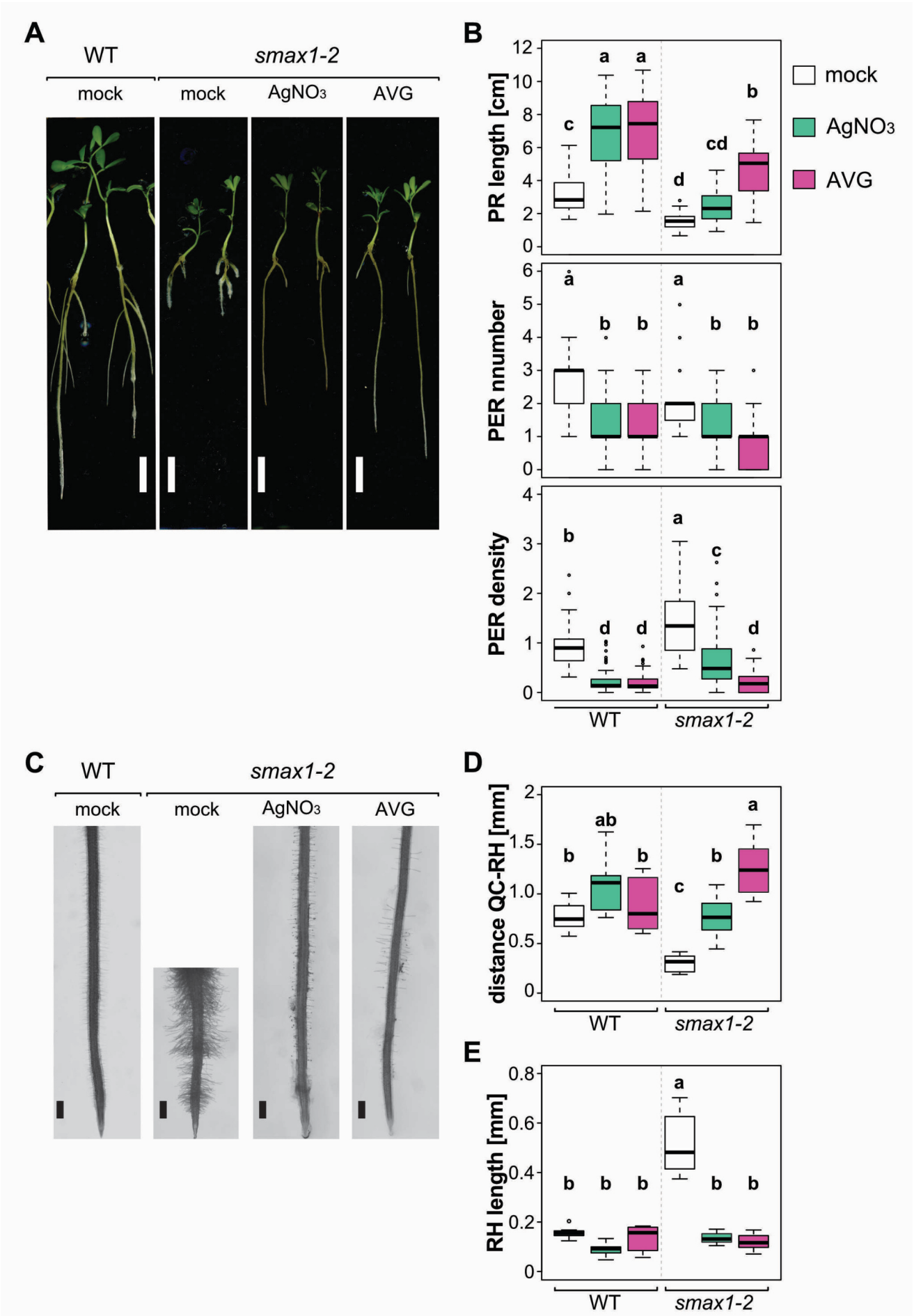

Fig. S18. Rescue of the *smax1-2* root and root-hair phenotypes by ethylene signaling inhibition. **(A)** Representative images (scale bar = 1cm) and **(B)** quantification of primary root (PR) length, post-embryonic root (PER) number, and PER density of 10-day-old wild type and *smax1-2* seedlings grown in presence of 50μM silver-nitrate or 0.1μM AVG (n ≥ 24). **(C)** Representative images of the root tip (scale bar = 500μm), **(D)** distance between the first root-hair (RH) and the quiescent-center (QC), **(E)** and the RH length of wild type and *smax1-2* in presence of 50μM silver-nitrate or 0.1μM AVG (n ≥ 7). **(B, D, E)** Letters indicate significant differences (ANOVA, post-hoc Tukey test).

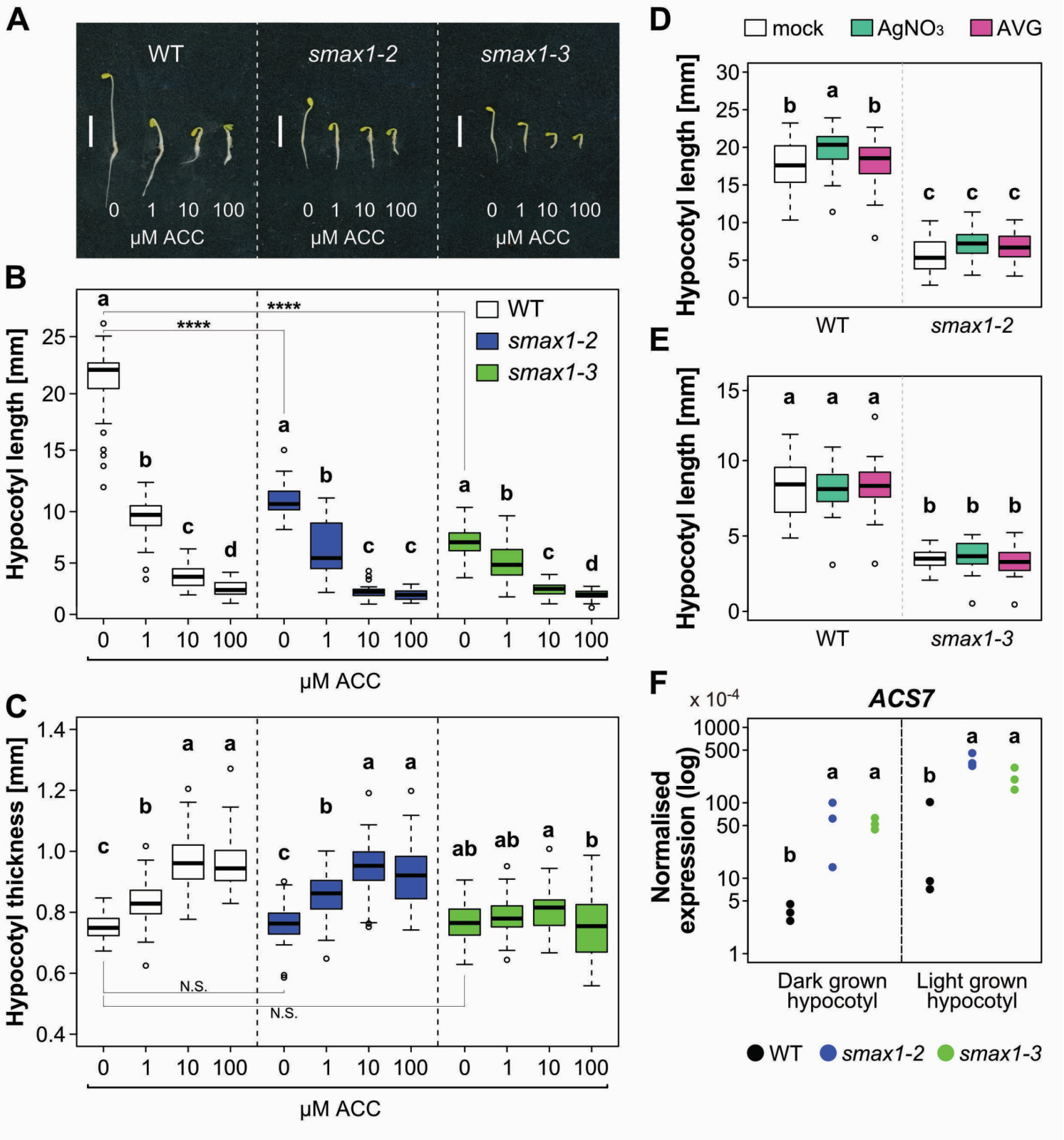

Fig. S19. Elevated ethylene biosynthesis is not causative for the short hypocotyl of *smax1*. **(A-C)** Triple response assay, for which seedlings were grown in the dark for 4 days with the indicated ACC concentrations (n = 40). Scale bar = 1 cm. **(D-E)** Hypocotyl length of wild type and *smax1* mutants when grown in a 16h/8h light cycle for 2 weeks days in presence of 50µM silver-nitrate or 0.1 µM AVG (n ≥ 40). Plants used for hypocotyl measurements were the same as used for PR length measurements in Fig. 4C **(D)** and Fig. S17 **(E)**. **(F)** Normalized transcript accumulation of *ACS7* in hypocotyl tissue grown in the dark for 4 days or 16h/8h light cycle for 10 days (n = 3) as determined by RT-qPCR. Expression values were normalized to the expression of *Ubiquitin*. **(B-C)** Asterisks indicate significant differences between mock treated genotypes (ANOVA, post-hoc Dunnett test, N.S.>0.05, ****≤0.0001). **(B-F)** Different letters indicate significant differences (ANOVA, post-hoc Tukey test).

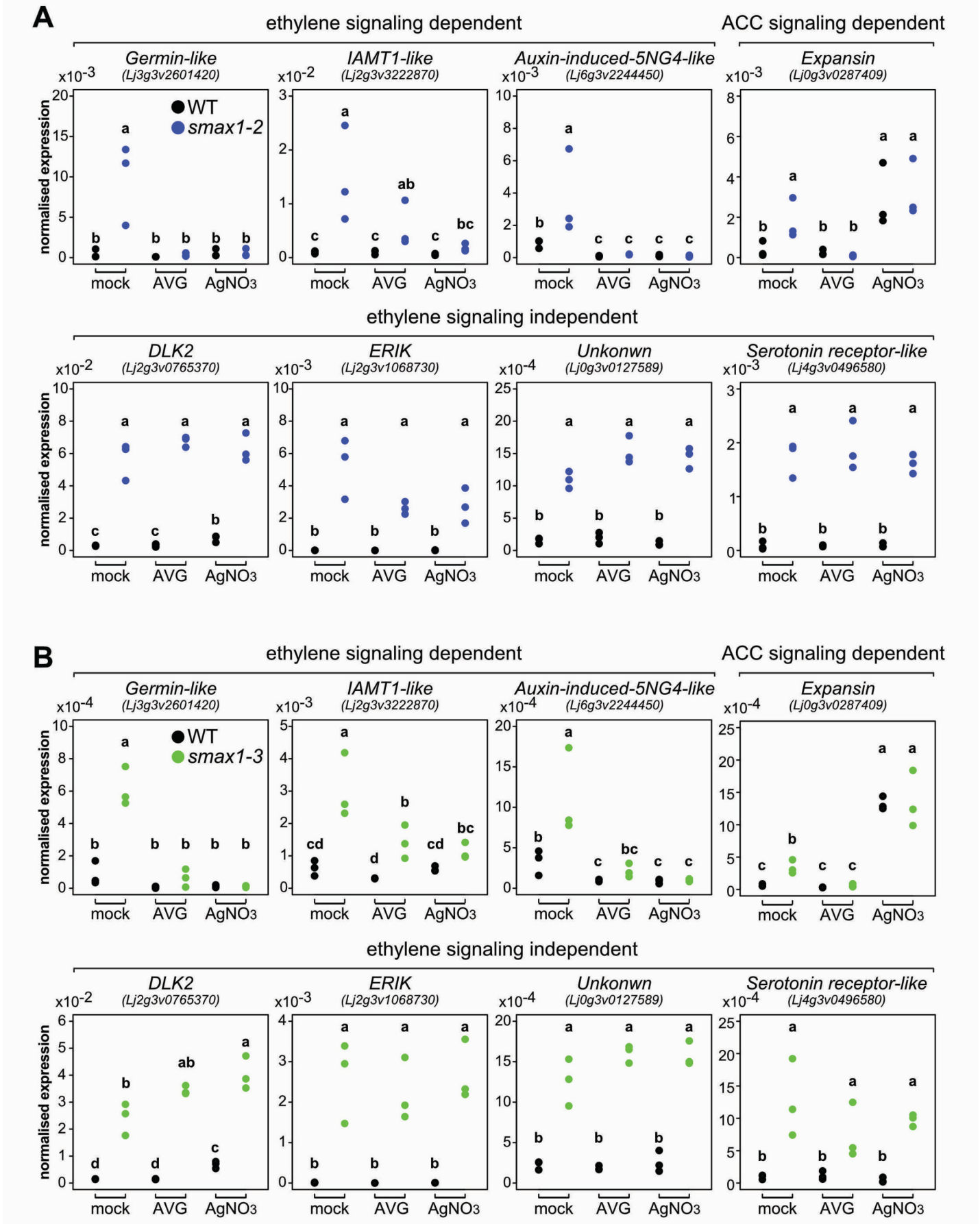

Fig. S20. Ethylene signaling-dependent and -independent DEGs in *smax1* mutants. **(A-B)** Transcript accumulation as determined by RT-qPCR of indicated genes in roots of wild type, **(A)** *smax1-2* and **(B)** *smax1-3* grown on 0.1µM AVG or 50µM silver-nitrate (n = 3). Expression values were normalized to the expression of *Ubiquitin*. Different letters indicate significant differences (ANOVA, post-hoc Tukey test).

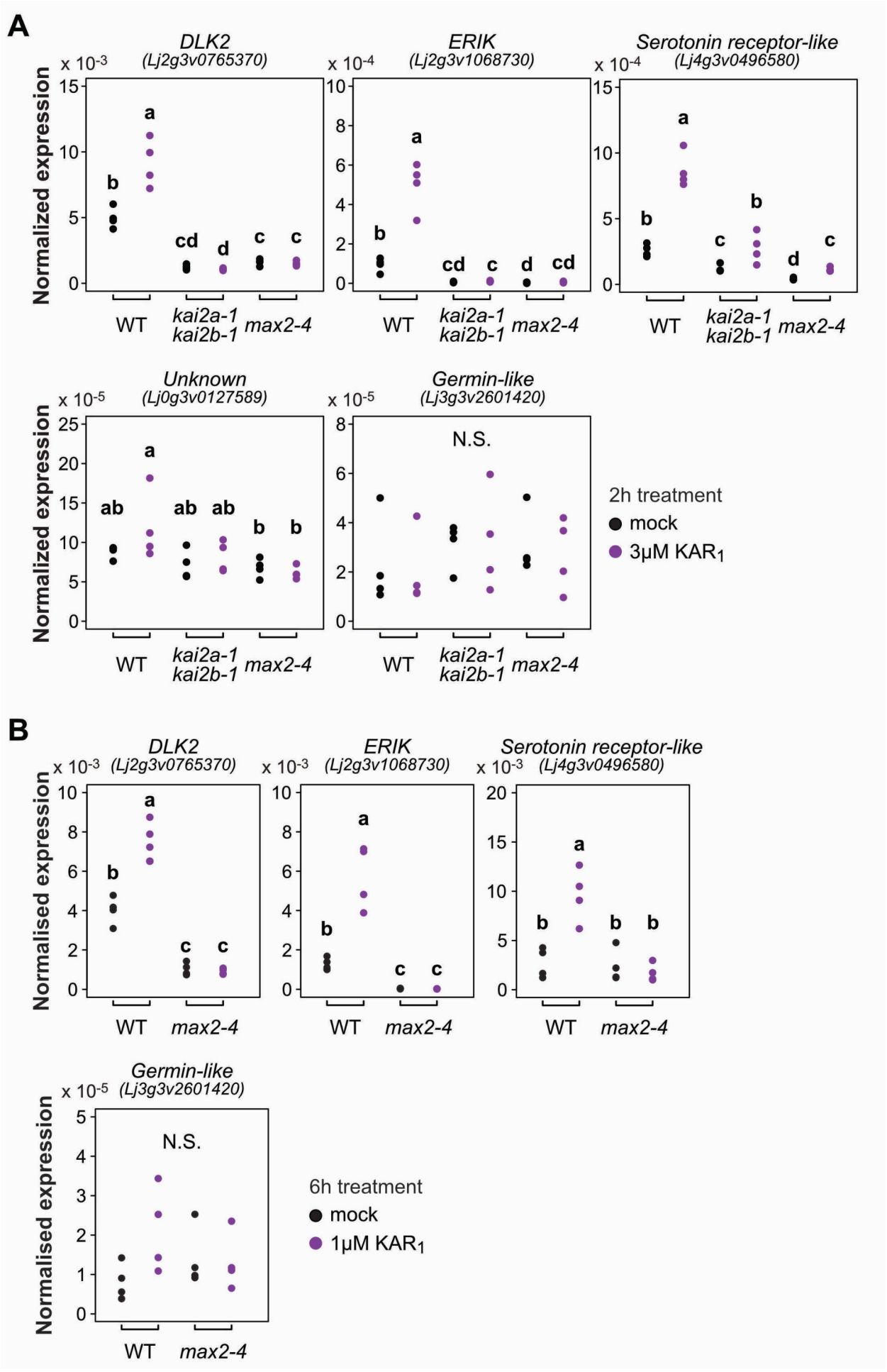

Fig. S21. Ethylene-independent DEGs respond rapidly to KAR_1 treatment. **(A-B)** Transcript accumulation as determined by RT-qPCR of indicated genes in the indicated genotypes, **(A)** after 2 hours treatment with 3μM KAR_1 (n = 4), **(B)** after 6 hours treatment with 1μM KAR_1 (n = 3). Expression values were normalized to the expression of *Ubiquitin*. Different letters indicate significant differences (ANOVA, post-hoc Tukey test).

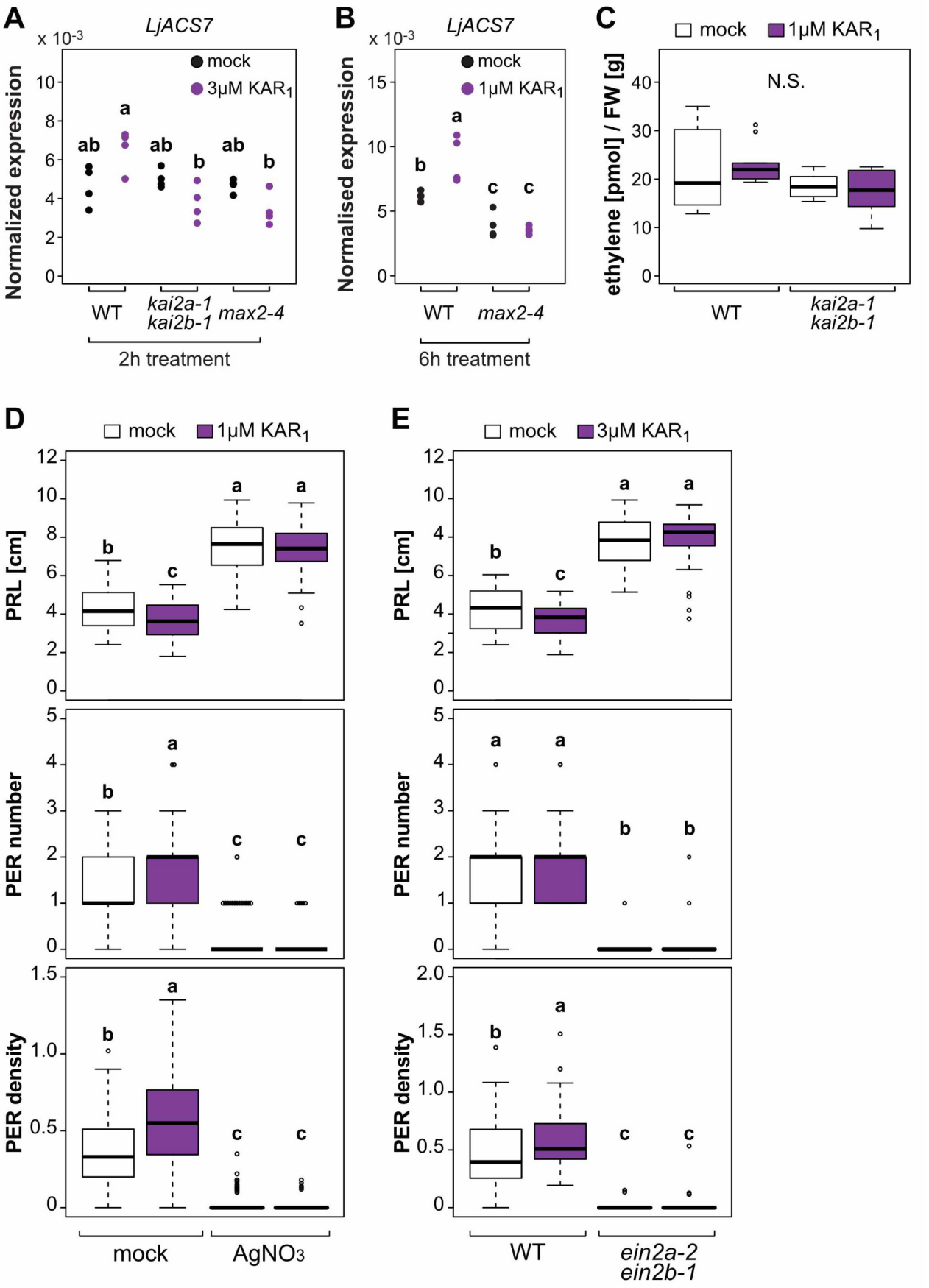

Fig. S22. Ethylene signaling is required for root developmental response to KAR_1. **(A-B)** Transcript accumulation of *ACS7* in wild type roots after **(A)** 2 hours treatment with 3μM KAR_1 (n = 4) or **(B)** 6 hours treatment with 1μM KAR_1. Expression values were normalized to the expression of *Ubiquitin*. **(C)** Ethylene released by *L. japonicus* wild type and *kai2a-1 kai2b-1* seedlings and in response to treatment with 1μM KAR_1 as determined by gas chromatography (n = 8-9). **(D-E)** Primary root (PR) length, post-embryonic root (PER) number, and PER density of 10-day-old **(D)** wild type seedlings co-treated with 1μM KAR_1, equal amounts of solvent and/or 50 μM silver-nitrate (n ≥ 57), and **(E)** seedlings of wild type and the ethylene insensitive mutant *ein2a-2 ein2b-1* grown on 3μM KAR_1 (n ≥ 29). Letters indicate significant differences (ANOVA, post-hoc Tukey test).

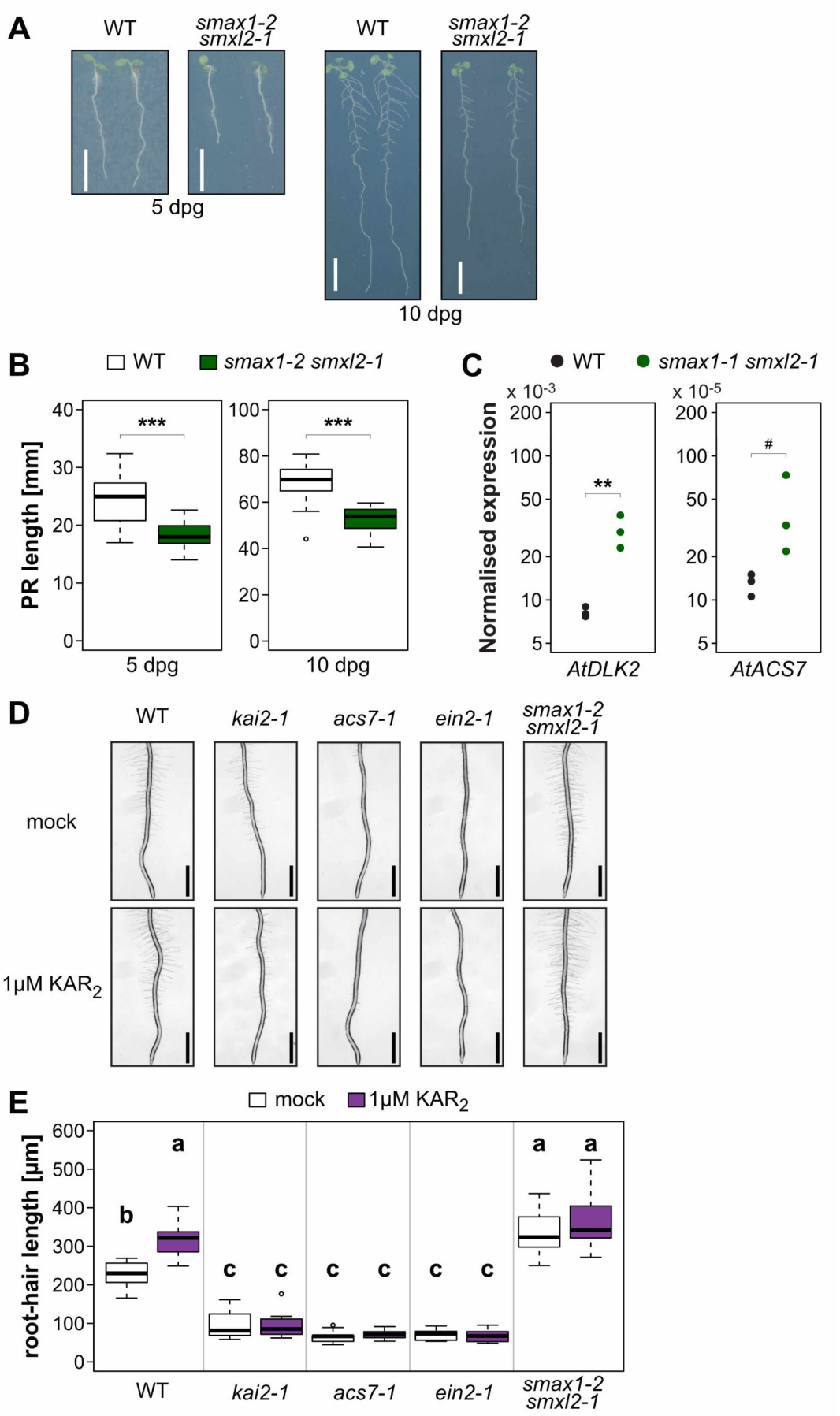

Fig. S23. Induction of *Arabidopsis thaliana* root hair growth by KAR depends on *ACS7*. **(A)** Representative images of primary roots (scale bar = 1cm) and **(B)** primary root (PR) length of *A. thaliana* wild-type and *smax1 smxl2* at 5 and 10 days post-germination (n = 20). **(C)** Transcript accumulation as determined by RT-qPCR of *DLK2* and *ACS7* in roots of *A. thaliana* wild-type and *smax1 smxl2* normalized to the transcript accumulation of *EF1α* (n = 3). **(B-C)** Asterisks indicate significant differences between genotypes (Welch t-test, #≤0.1, *≤0.05, **≤0.01, ***≤0.001) **(D)** Representative images (scale bars = 1 mm) and **(E)** root hair length of 5 day old Arabidopsis seedlings of the indicated phenotypes treated with solvent or 1 µM KAR_2. 10 root hairs were measured per seedling (n = 8 to 10). Letters indicate significant differences (ANOVA, post-hoc Tukey test).